Georgia Tech Sponsored Research

9

Project	E-20-E82 F767
Project director	Frost (James David)
Research unit	CEE
Title	Concrete Building Materials Microstructural Damage and Quanttification
Project date	1/31/2000

E-20-682

PROJECT SUMMARY

DoD USAF SBIR PHASE I FINAL REPORT

Project No: **AF99-190** Contract No: F08630-99-C-0063

PROJECT TITLE: Concrete Building Materials Microstructural Damage and Quantification

NAME AND ADDRESS OF OFFEROR

Dr. A. B. Thakker, P.E.
Global Technology Connection, Inc.
P.O. Box 669696
Atlanta, GA 30066

SUMMARY

This project demonstrated the feasibility of using recent advances in image analysis for studying concrete materials at micro scales and using quantitative measurements obtained with these methods to provide new insight into the macro-scale behavior. Phase I dealt primarily with development of visualization and quantification techniques including sample preparation and schematic of data reduction software for concrete microstructure. More specifically, a sample preparation technique has been developed to create high quality coupon surface that permits unambiguous detection of voids, microcracks and other features. The sample preparation techniques developed include a combination of grinding, polishing, epoxy coating, image filtering and bright field imaging. State-of-art techniques including image montage and serial sectioning, which allow for generation of high resolution 3D images of large area and volume, have been successfully adapted to the concrete microstructural damage quantification in this project. Automated data reduction software including those for the quantification of the damaged specific surface area tensor, mean solid tensor, local volume fraction, fractal dimension etc. have been also successfully adapted for this application. General qualitative observations on both concrete and the projectile material, and quantitative determinations of the microstructural characteristics of concrete using theses techniques have been also completed.

The overall goal of the proposed phase II program is to apply the techniques developed in Phase I to develop low cost, commercially viable experimental technology and computerized automated data reduction package that can relate concrete micro-structural attributes to effective mechanical properties. It is envisioned that this development will have wide applications in both military and civilian research and development, and commercial services such as damage evaluation of ballistic penetration, damage assessment due to earthquake and explosion, forensic study and concrete mixture design.. Commercialization of this technology as well as third party funding will be emphasized throughout the program. An optional task (Phase II) for improving understanding of penetrator material degradation, deformation, design, and penetrator-concrete interaction is also proposed.

The result of this project will be widely applicable to:
USAF(Munitions) and other DoD Components
Government agencies(Corps of Engineers, Federal Highway Administration)
Ammunition Manufacturers
Concrete Material users /producers
Geo-Material users/producers
Construction Industry
Earthquake/Hurricane Damage Assessment(Insurance Companies)
Life Prediction and Durability Assessment of Concrete and Geo-Materials
Pavement Mix Durability Enhancement
Aggregate Particle Sizing and Shape Measurement

SUBMITTED BY: A. B. Thakker DATE: Feb 15, 2000
Principal Investigator Signature

TABLE OF CONTENTS

I PHASE I PROJECT OBJECTIVES

The overall goal of this SBIR is to develop economic, automated, imaging based experimental techniques for quantification of relevant concrete micro-structural artifacts and to relate these micro-structural quantities to conventional macro-scale properties such as strength and modulus. To achieve this goal, Phase I of the project focussed on identifying, adapting, and implementing techniques which could be used to quantify the inherent micro-structure (far-field "as-prepared" concrete microstructure) as well as the induced micro-structure (near-field microstructure resulting from penetration events). An integral part of identifying appropriate techniques was the need to be able to quantify microstructure at multiple scales because of the multi-dimension multi-constituent nature of concrete and the concomitant multi-scale damage resulting from the penetration event.

To achieve the Phase I objectives, the following five tasks were designed:

1. Develop sample preparation techniques that will allow the unambiguous detection of various microstructural artifacts, acquisition and processing of best quality images. This task is of paramount importance for the measurement of various features.

2. Develop special image acquisition techniques for sampling large area and large volumes so that microstructural quantities thus obtained are statistically meaningful. Montage creation and serial sectioning are the two state-of-art techniques that allow for sampling large area and volume to obtain high-resolution images.

3. Identify the microstructural quantities that most effectively represent the type and level of damage. For different applications, the controlling microstructural quantities may not be the same. A thorough literature review is effective in identifying the causes of these microstructural damages and their influence on macro properties.

4. Develop automated data reduction software so that the identified microstructural quantities can be efficiently computed.

5. Demonstrate the quantification of microstructural damage in the provided penetration target by applying the newly developed or adapted techniques.

II INTRODUCTION & MOTIVATION

It is well recognized that material microstructures determine its macro properties. However, to detect, quantify microstructures and relate them to macro properties is a challenge to material scientists. Concrete is a multiple-component composite comprised of various constituents and especially damages at different length scales. Studies have shown the direct influence of the microstructural damage parameters on the macro properties of concrete, the integrity of concrete structures, and the penetrability of concrete by projectiles. In recent years, breakthroughs in techniques for visualizing (imaging techniques) microcracking and void distribution and determining these quantities make it possible to take this challenge. In this regard, development of a low-cost, experimentally based process to quantify microstructural damage in concrete, and a computer software for automated and efficient data reduction is of primary importance. Once developed, these techniques can be utilized efficiently in correlating common material properties such as strength and modulus to the microstructural parameters. These are actually the objectives identified in the request for proposals for Phase I and Phase II research.

For image analysis applications, the importance of obtaining high-quality images can not be overemphasized. Poor-quality images not only result in inaccuracy but can yield entirely misleading information (Marusin, 1995, Jang et al., 1999). In the Phase I study, a major focus was put on exploring and developing specific methodologies to ensure high quality images from which the necessary quantitative measures could be obtained. Effort was also expended on implementing automated image processing software for determining the microstructure quantities identified to be relevant for quantitative correlation with critical effective concrete properties. Previous experience has routinely indicated that as long as image quality and automated image processing objectives can be properly achieved, specific objectives such as quantification of the damage caused by penetration events can be accomplished both efficiently and accurately.

Microstructural damage in concrete involves different length scales ranging from nanometer to centimeter. To obtain statistically meaningful quantities, sampling size is an important issue. In order to detect microstrucral damage at small scale, a large magnification is needed and one image will cover a small area in this situation. Therefore a statistically meaningful sampling could be obtained only by acquiring multiple images at high resolution and accurately align them together. This technique is called image montage and will be adapted to the application in this project. Equally important is the measurement of the distances of nearest neighbors, which are critical in accounting for the microdamage interaction. The nearest neighbor distance, as has been demonstrated, can not be accurately measured from two dimensional sections. It is therefore important to reconstruct three dimensional microstruture through serial sectioning over a large representative volume . Use of serial sectioning and montage creation developed by members of this project team will enable multi-scale high resolution quantification of microstructural damage for large areas and volumes of concrete.

Portland cement concrete is a brittle material, which is actually determined by the properties of its constituents: aggregates, paste, and various distributed discontinuities such as voids, pores, cracks, and interfacial transition zones (ITZ). Therefore the volumetric density of these features and their spatial and orientation distribution are important. In recent years, continuum damage mechanics, fracture mechanics and micromechanics have developed to the stage where engineering application becomes feasible. These branches of mechanics develop analytical relations between material macro properties such as strength, modulus and the microstructural features. A thorough evaluation of these relations will help identify the quantities that have significant influences on macro properties and ensure that reasonable correlation in the Phase II study.

III PHASE I RESULTS

A. TASK 1: SAMPLE PREPARATION TECHNIQUES

A variety of surface preparation techniques were utilized during Phase I on coupons cut from both a 4" diameter core recovered from near the edge of a tested 30" diameter target as well as from a 7.5" diameter core which was obtained from near the center of the same tested target. The 7.5" core contained a tunnel which had been resin filled before the specimen was cored. It was considered that the 4" diameter core would more closely reflect a concrete with an inherent microstructure (microstructure that only reflected curing environment) while the tunnel core would clearly have an induced microstructure (due to penetration test) in addition to an inherent one. It is noted that part of one of the tasks proposed herein for Phase II is to investigate whether a 4" diameter core from near the edge of an untested target and a 7.5" diameter core obtained from the center of an untested target have the same inherent microstructure. It is anticipated that there may be some differences due to small differences in curing conditions at the edge of a large specimen versus the edge of the same specimen. For the purpose of evaluating alternative surface preparation methods during Phase I, the 4" core was considered to be reasonably reflective of an induced microstructure only.

The purpose of examining alternative surface preparation techniques during Phase I was to identify procedures which would allow for the highest quality images to be captured while at the same time minimize the amount of manual processing required on the captured images since this can quickly dictate the efficiency of the overall process of microstructure quantification. In addition, since it was known that features of different sizes are relevant to the overall process, consideration was given to the multi-scale nature of the problem in order to determine the optimal procedure for preparation of coupon surfaces and hence quantification of various components of the concrete microstructure. A number of techniques, each of which required different levels of effort were evaluated. For each of these preparation techniques, a number of images were captured at various levels of magnification. For purposes of comparison, this summary deals primarily with images captured at 25X magnification.

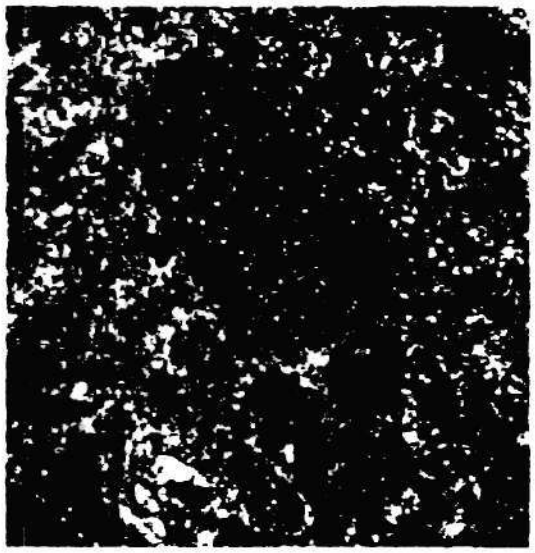

Figure 3.1.1 Image of Unprocessed Cut Surface at 25X

Cut Surface, No Preparation

Coupons for use in image analysis are typically cut from a larger specimen (concrete core in this case) with some form of slab or diamond circular saw. An image of the surface of one such coupon at 25X magnification without further preparation is shown in Figure 3.1.1. Light reflecting off the rough surface causes small white flecks to appear on the surface of the coarse aggregates. Although a small almost circular void is detectable by eye just beneath the largest aggregate, unambiguous detection of other features would clearly be difficult.

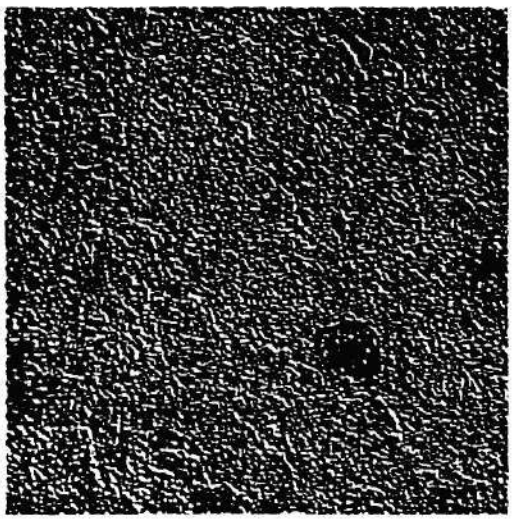

Figure 3.1.2 Enhancement of Void

Image Filtering

Since the voids are depressed from the surface of a coupon, a CCD camera focussed on the surface will not be focussed on the interior of the void and this causes the void space to appear somewhat blurred in an image. It is possible to take advantage of this type of feature through image filtering techniques. If the image in Figure 3.1.1 is taken through a process of edge enhancement and embossing, the void space will appear as a relatively smooth uniform gray scale portion against an otherwise variable surface, as shown in Figure 3.1.2. This can provide a rapid way to identify voids and to make estimates of the number of voids and the void ratio of an image.

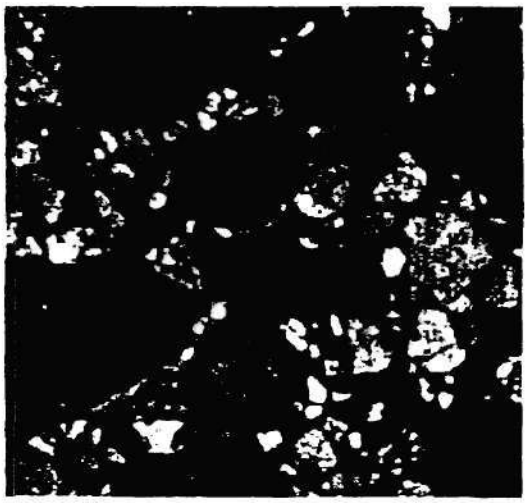

Figure 3.1.3 Image of Concrete at 25X

Grinding

Grinding procedures help smooth the coupon surface so that the various phases of the concrete matrix can be more easily distinguished. Factors that can be varied include rate and duration of grinding and the characteristics of the grit used. For the present study, grinding using a platen rotating at 120 RPM for 10 minutes each with 60-grit, 120-grit, 240-grit, 400-grit, and finally 600-grit sandpaper was found to yield very good quality images. For example, the image in Figure 3.1.3 shows a surface at 25-X magnification after completion of the grinding process. The surfaces and edge boundaries of both coarse and fine aggregate are more clearly distinguishable after grinding. Again, the void space is detectable based on its circular shape.

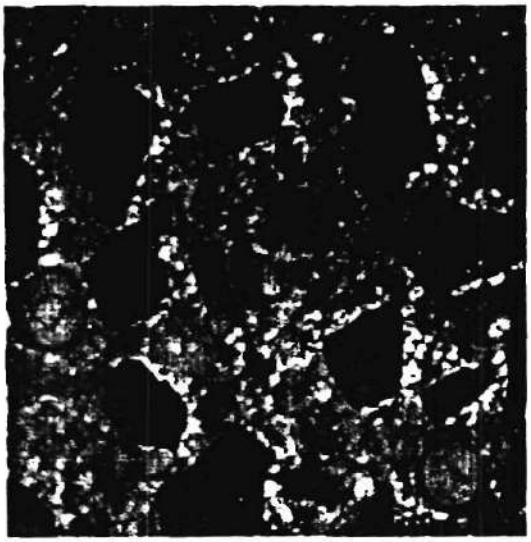

Figure 3.1.4 Image of Concrete at 10X

The same surface at 10X magnification is shown in Figure 3.1.4. In this case, due to the larger field of view, it is possible to detect void of different sizes over a range of scales. In some of the voids a "lip" effect is evident. This indicates that the grinding procedure may remove material around the edges of the void space, which would result in an overestimate of the void size and hence the void ratio.

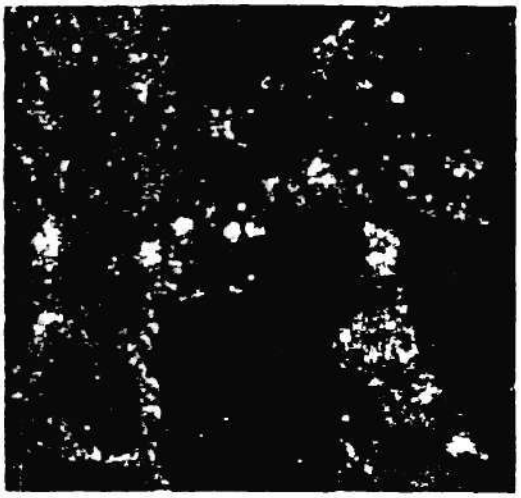

Figure 3.1.5 Image of Epoxy-Coated Concrete at 25X after Grinding

Figure 3.1.6 Reflection of Light from Resin Filled Void

Epoxy Coating and Subsequent Grinding

To prevent the unwanted removal of material noted above, the concrete surface was coated with an epoxy after cutting but before the complete grinding process was performed. The image in Figure 3.1.5 shows an epoxy-coated surface at 25X magnification after the complete sanding procedure. Note that the void in the center of the image is still distinguishable from the coarse aggregate based on its circular shape and its lighter, gray color. However, the color is very similar to some of the finer aggregate particles. It is preferable to distinguish the voids based on color since that process can be performed automatically by computer more easily than detection based on shape (this can be done more easily for simple shapes – e.g. relatively circular objects such as pores or relatively long objects such as fissures).

Polishing

Following the multi-grit grinding procedure described above, the epoxy-coated surface was polished, again with the platen rotating at 120 RPM, for 10 minutes each with a 9-μm and a 6-μm diamond powder. The resulting image at 25X magnification is shown in Figure 3.1.6. Here the epoxy-filled voids are clearly distinguished from the rest of the concrete microstructure due to the intensity of light reflected off their highly-polished surfaces. Even though all phases on the surface of the coupon are subjected to the same grinding and polishing processes for the same duration and under the same pressure, the relative hardness of the phases means that under the brightfield microscopy light system used by the proposers, only the softer resin in the pores is reflecting the light. The other harder surfaces diffuse the incident light due to micro-scratches caused by the diamond paste used in the polishing stage.

General Observations Based on Multi-Scale Evaluations of Dissected Cores

At the same time as identifying surface preparation procedures for use in Phase II of the project, observations were made at a number of scales to help determine any specific needs of the project. A number of key observations that played an important role in planning the Phase II tasks are described below. In particular, these studies focussed on analyzing the surfaces of coupons cut from the 7.5" core containing the tunnel. Three-quarter-inch thick discs were cut from the core orthogonal to the path of the projectile. Thinner discs were found to be somewhat unstable due to damage resulting from the penetration test. The two cut surfaces of each disc were first made parallel and smooth at the macro-level, to ensure uniform polishing and to facilitate microscope examination. This was accomplished using a Harig 618 Autostep Grinding Machine (Figure 3.1.7). After detecting the thinnest point on the disk, the machine was programmed to trim the entire disk to the minimum thickness, with a precision of .001". The grinding wheel is relatively coarse (~60 grit).

Figure 3.1.7. Automated Grinding

At this point, without further specimen preparation, a number of observations can be made, at both the macro- and meso-scales. To the naked eye, the tunnel appeared circular, with a diameter of approximately 0.5". The circular region extending up to about 1.0" from the tunnel boundary had a different coloring, perhaps due to the displacement of cement by the harder aggregate particles, as well as increased density of coarse aggregate due to particle crushing. There were no observable voids of any significant size (> 1/16") in this region, whereas voids of approximately 1/8" diameter were common and uniformly distributed throughout the rest of the specimen.

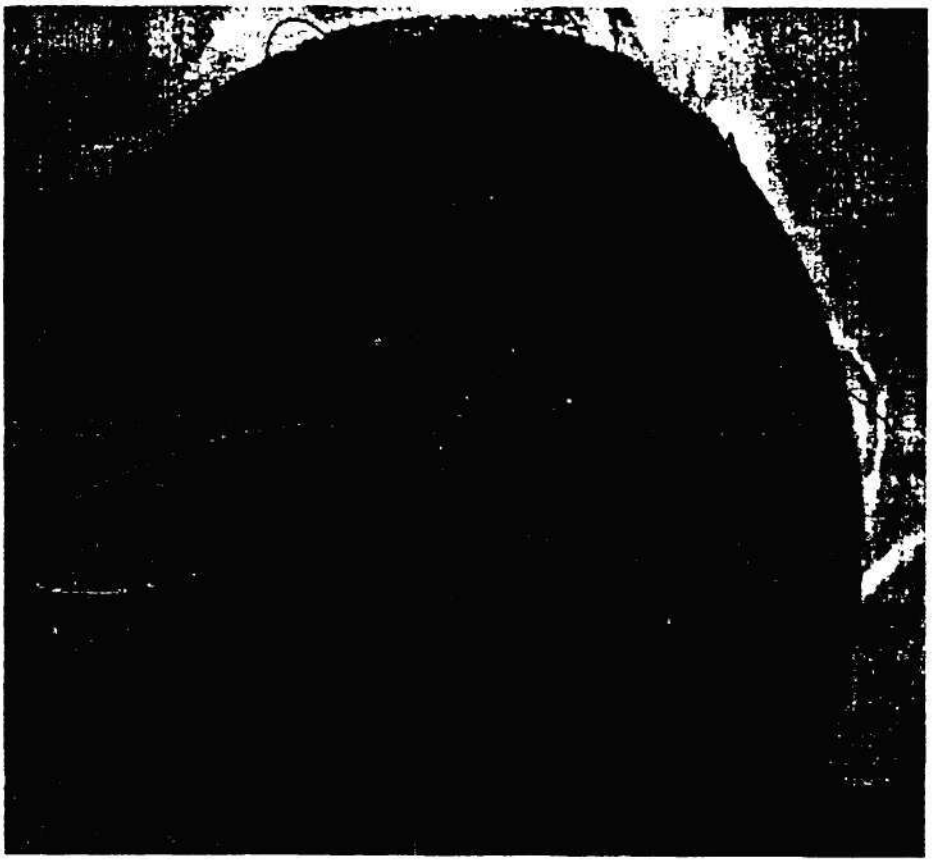

Figure 3.1.8. Disc Cut from Tunnel Core showing Macro-Scale Cracking and Resin-Filled Tunnel

There are five observable crack groups in the specimen shown in Figure 3.1.8. Each begins within 1 inch of the tunnel boundary and extends all the way to the specimen edge. Cracks A and B, in the figure above, are significantly larger than the other three. Cracks A, C, and E are single cracks. Crack B splits into two at a point approximately 1 inch from the tunnel boundary. In Crack C, two small cracks merge into one at a point approximately 2.5 inches from the tunnel boundary. The origin/genesis of these cracks is thought to be dictated, at least in part, by the target boundary conditions and is the focus of one of the proposed Phase II tasks.

Preliminary microscopic examination was also conducted at this level of preparation. The tunnel was injected with resin before sampling, and is shown at 25X magnification in Figures 3.1.9. (The horizontal lines on the epoxy surface are an artifact of the initial grinding procedure.) The tunnel shape is shown to be significantly impacted by the presence of coarse aggregate and fine aggregate. The bottom border of the tunnel appears to conform to the edges of a quarter-inch long piece of coarse aggregate, while the top edge depicts two sand particles, approximately 1/25" in diameter, that protrude into the tunnel path.

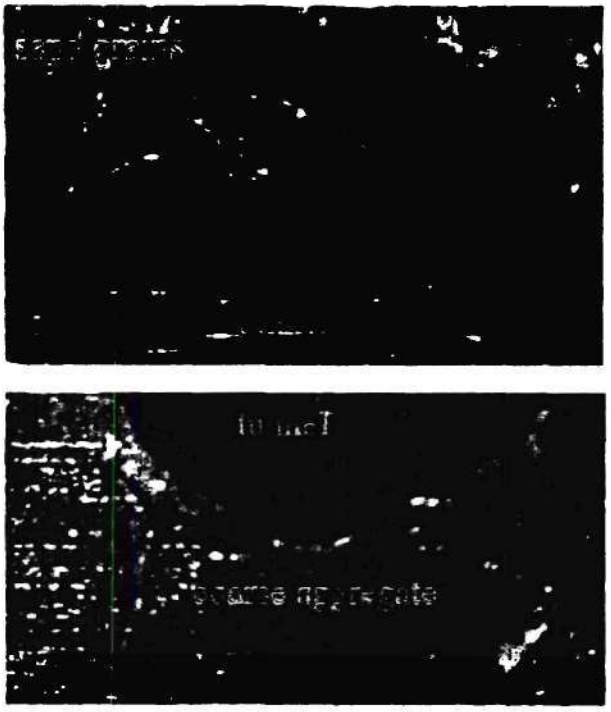

Figure 3.1.9. Influence of Coarse and Fine

The range of crack widths observed at this minimal level of preparation is depicted in the images in Figure 3.1.10 (both at 10X magnification) taken at a distance of approximately 2" from the tunnel boundary. The top image shows Crack B (Figure 3.1.8), which ranges up to about 1/10" wide. In contrast, Crack E is shown below it, at the same level of magnification, and is narrower by about one order of magnitude. The exact borders of the cracks at the surface are difficult to determine at this level of preparation.

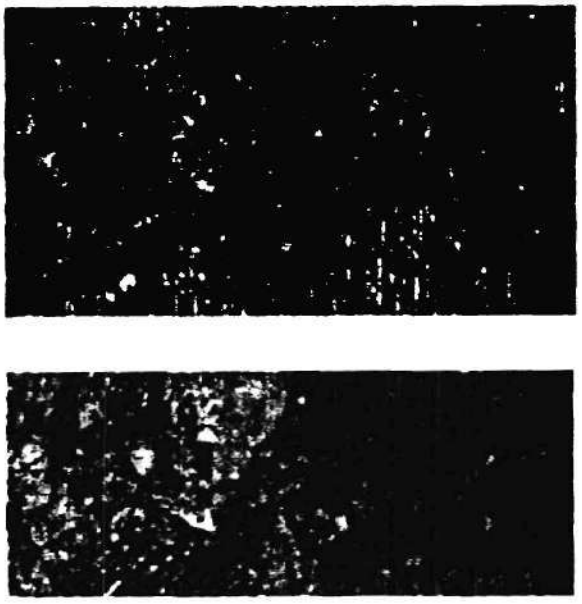

Figure 3.1.10. Images of Cracks in Different Widths in Concrete

Two further observations can be made about the damage at this level of preparation: Crack growth appears to be facilitated by the presence and proximity of voids. The left image in Figure 3.1.11, taken at 25X magnification, show a crack extending between two circular voids. Also, cracks tend to travel along the boundary of coarse aggregates, indicating that crack growth is facilitated by poor bonding between aggregate and mortar. The right image in Figure 3.1.11 shows a crack traveling between two aggregate particles, both of which have been de-bonded from the adjacent mortar. Accordingly, it is evident from this macro-scale assessment that a range of crack propagation mechanisms exist. The degree to which any one mechanism will contribute to the overall induced microstructure

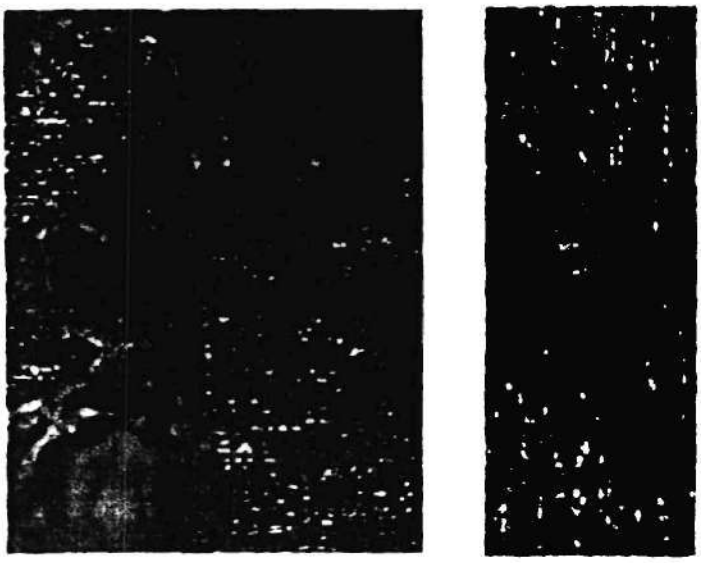

Figure 3.1.11. Images showing Alternative Crack Propagation Mechanisms

through aggregate particles.

To enhance the quality of images, the surface of the disc was coated with epoxy and then subjected to the grinding and polishing procedures described earlier. This greatly facilitated the detection of coarse aggregate, mortar, and void/crack space, even with minimal magnification. For example, the upper image in Figure 3.1.12 (10X magnification) shows epoxy-filled void and crack space clearly distinguishable from the rest of the concrete mixture based on gray color.

Higher magnification reveals many of the same observations described earlier. The lower image in Figure 3.1.12 (25X magnification) shows Crack C (refer to Figure 3.1.8) propagating through a circular void at a point approximately 1.5" from the tunnel boundary. At its narrowest point, this crack is approximately 1/200" wide. This image clearly shows the interaction that occurs between aggregates, voids and cracks. It is noted that the upper fracture (Crack 1) traverses across the upper part of an aggregate particle just to the left of the main void. Due to the presence of epoxy and the surface is likely to be reflective of the inherent microstructure. For example, if the distance or mean-free path between air voids is large, then the potential for cracks to propagate through voids will be low. Similarly, if a crack is propagating in a particular orientation and encounters a zone of coarse intact aggregates, it is likely that the crack will propagate in the interface zone between the aggregates rather than through the aggregates. On the other hand, if the aggregates are weakened by pre-existing cracks, then induced cracks may traverse

Figure 3.1.12 .Polished Images showing Interactions between Aggregate, Void and Crack

preparation procedures identified in Phase I, the genesis of a much smaller crack (Crack 2) is also detectable in the image. These two cracks eventually join together at a distance of about 2" from the tunnel boundary.

At higher magnification, it is possible to clearly determine the crack boundaries and observe the cracking mechanism. Figure 3.1.13 (40X magnification) shows a crack propagating between coarse aggregates at a distance of approximately 2" from the tunnel boundary. It is seen to propagate along the edge of one piece of aggregate, completely debonding it from the mortar.

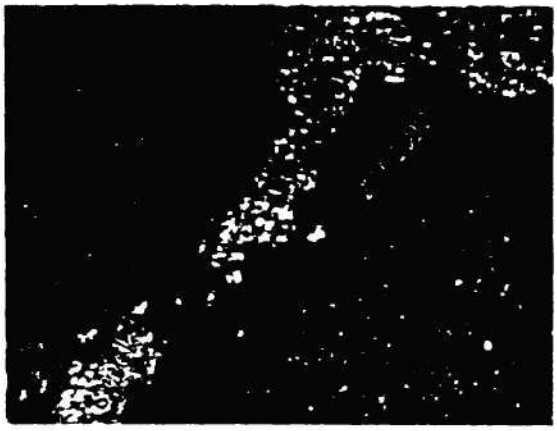

Figure 3.1.13. Crack Induced Debonding between Mortar and Aggregate.

At this high magnification it is also possible to observe different cracking mechanisms that are not visible without the use of epoxy and fine polishing. In the image shown in Figure 3.1.14, (40X magnification) which was taken at a point approximately 2" from the tunnel boundary, a very thin crack (~1/200") is shown to propagate through a piece of coarse aggregate. There also appears to be some separation between the aggregate and the mortar at the top left corner of the image.

Figure 3.1.14. Crack Propagating across Coarse Aggregate

It is clear from the general observations summarized above that in order to have sufficient detail to see the concrete microstructure features of interest, magnifications ranging from 10X to at least 40X will be required. The differences in behavior as a function of distance from the tunnel and images at higher magnifications (50X to 200X) will be presented in later sections.

It can be seen from the images discussed above that at magnifications of 10X to 40X, the details of the microstructure features of interest can be readily identified. On the other hand, it can also be seen that at these magnifications, the field of view in a single image does not contain a representative data set. Accordingly, the recently developed procedure of montage generation, whereby images at the desired magnification are stitched together to create representative fields of sufficient size at appropriate resolution will be used.

B. TASK 2: IMAGE MONTAGE AND SERIAL SECTIONING

Image montage is an important technique for sampling large area and volume at high resolution. For the measurement of certain quantities such as local volume fraction, specific damaged surfaces, one to three plane sections are needed for stereology based quantification. In this case, montage technique along will permit reasonably accurate determination of these quantities to meet the requirement based on statistical principles. For specific distance (nearest neighbor distance, not average distance) quantification, however, the combination of montage and serial sectioning is needed.

Image Montage: For image montage creation, a low-cost technique involves the use of pre-drawn grids. There are various techniques to pre-draw the grids, depending on the scale of interests. In the case of 1X to 40X magnifications, a grid generated by AutoCAD is satisfactory. The grid is first fixed to the coupon surface where images are to be acquired. The sample platform is then so moved that the image frame on the screen matches exactly with the grid frame. Figure 3.2.1 is an illustration of the procedures. Figures 3.2.2 and 3.2.3 are image montages thus created on a crater disk from the concrete sample of penetration test. Figures 3.2.2 and 3.2.3 presented 70 gray images and their corresponding binary images that cover a total area of 4cm by 12cm. These images were acquired at magnification of 15 with each image covering an area of 8mm by 8.6mm. The focus phase is crack and void. As each image is still at 15X magnification, small features can be clearly detected.

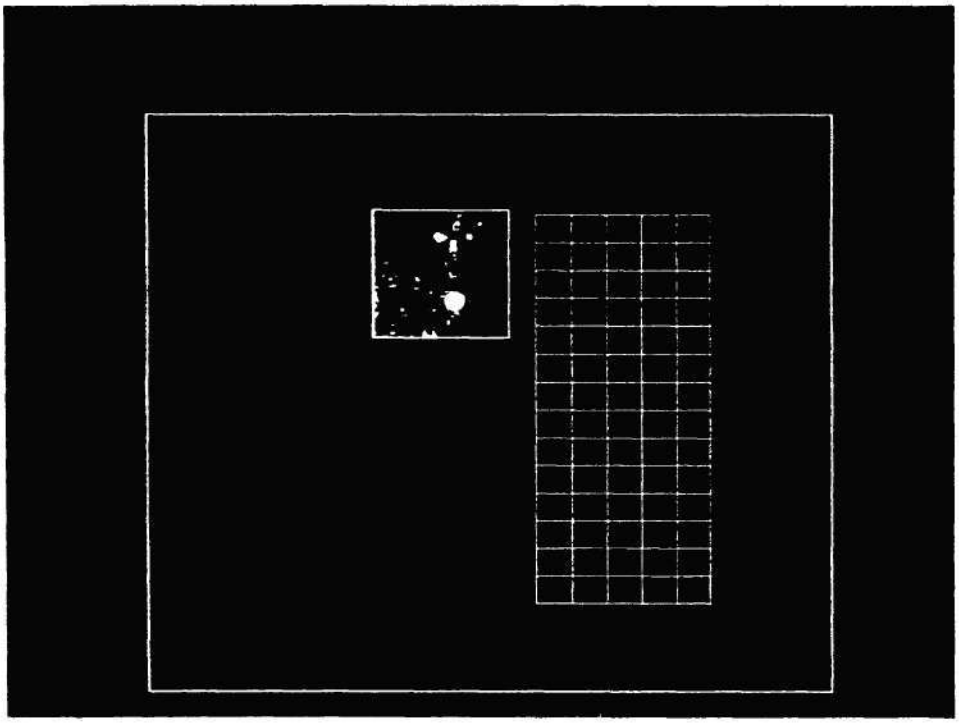

Figure 3.2.1 Illustration of Image Montage Acquisition Scheme

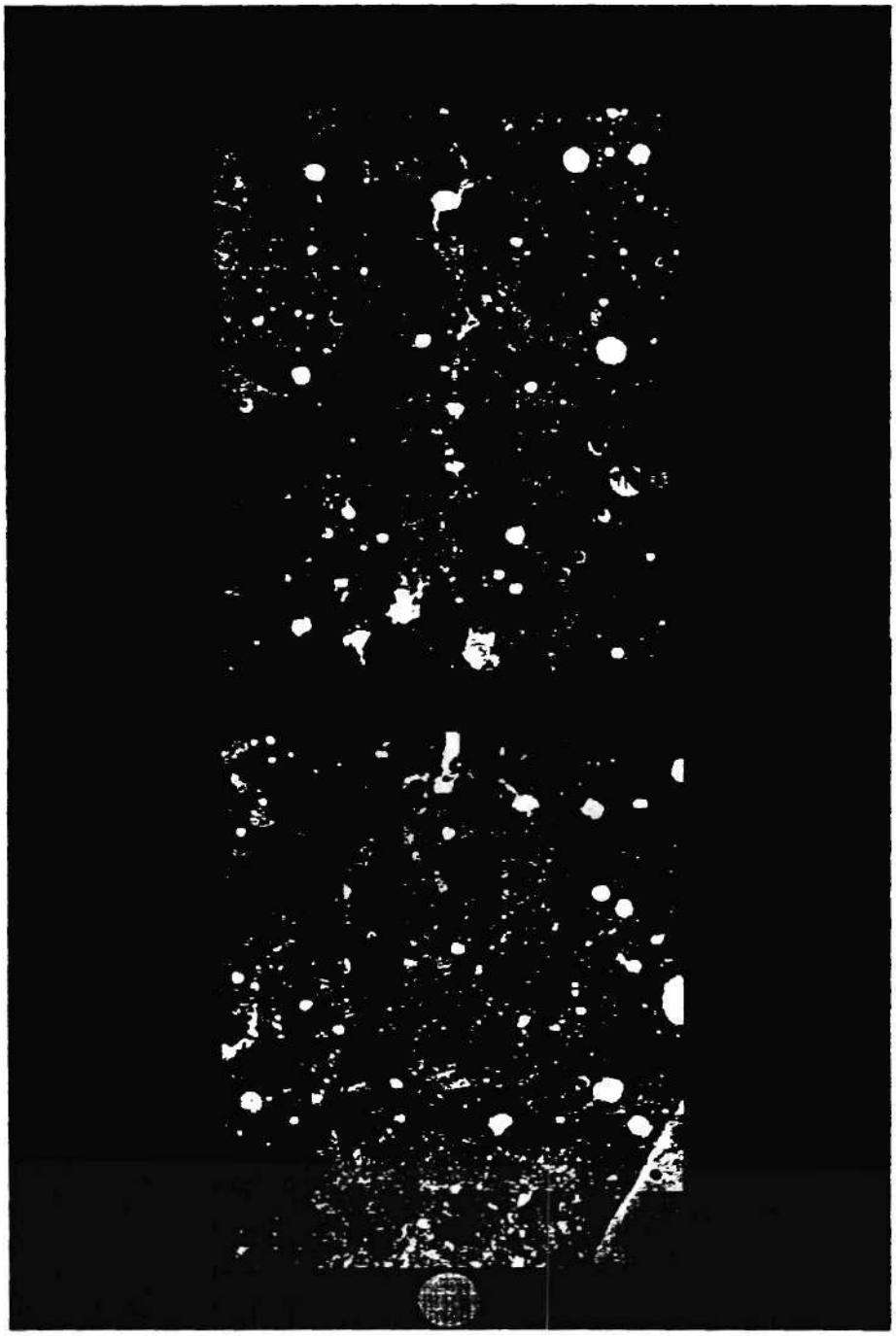

Figure 3.2.2 Image Montage Created from a Crater Disk

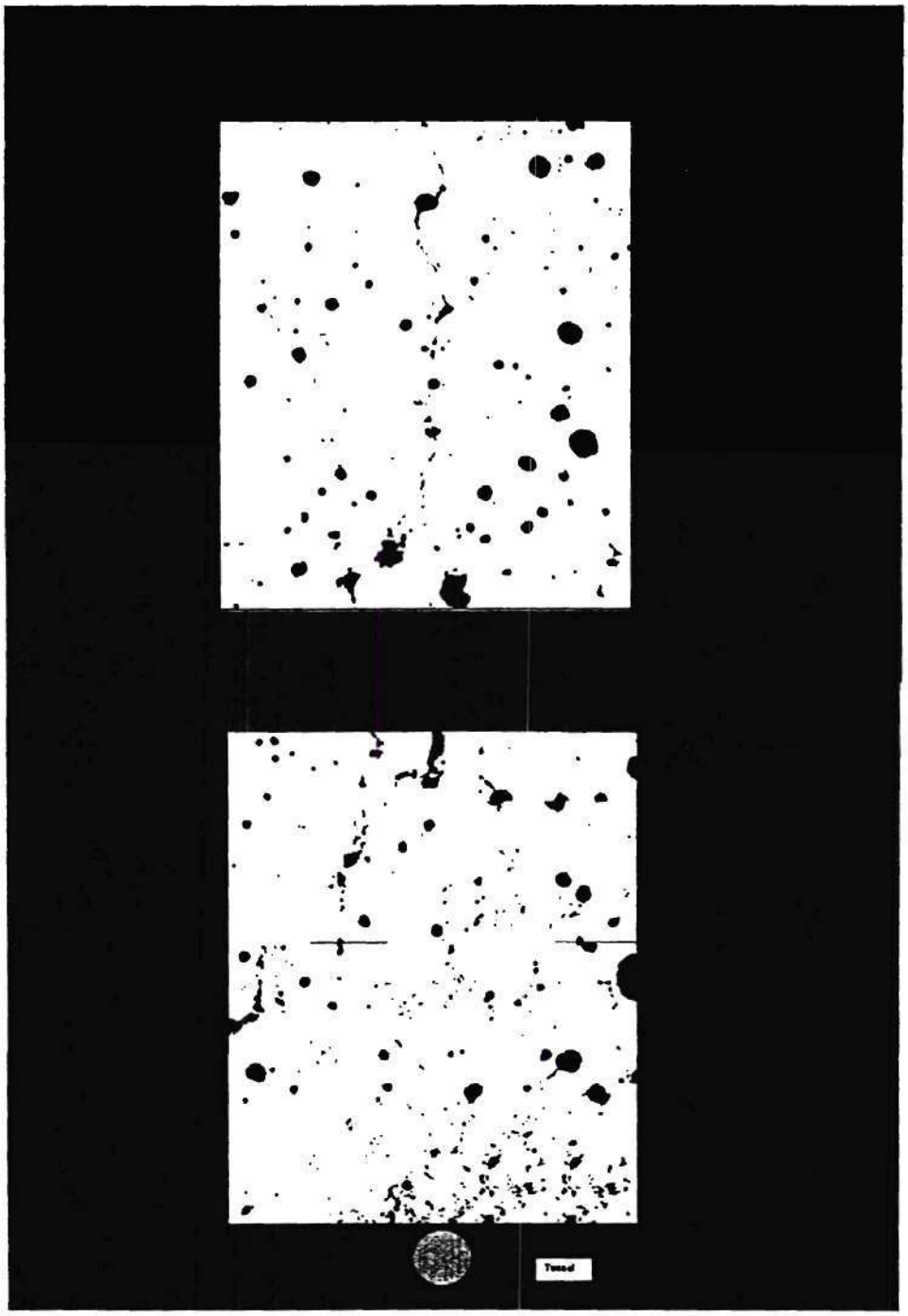

Figure 3.2.3 Image Montage Created from a Crater Disk

A special note concerning the selection of appropriate magnification is illustrated in Figure 3.2.4, where a crack appeared not connected under magnification 15X is actually a connected crack.

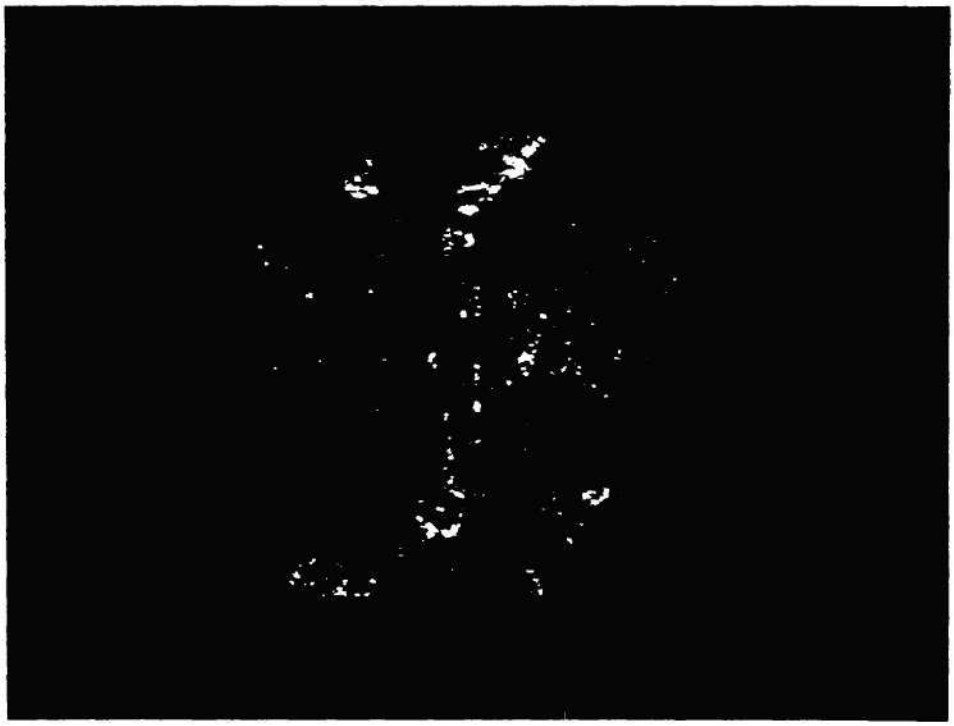

2.2.4 Illustration of Crack at Higher Magnification

Serial Sectioning

Due to the importance of serial sectioning in obtaining true 3D microstructural quantities, the algorithms, related problems and the methods that were developed by the members of the team were illustrated. This technique in combination with the montage creation implemented in the previous section will permit accurate 3D microstructural quantification. A microstructure (metal, concrete, or biological) is a collection of volumes, internal-surfaces, lines, and points. Depending on its dimensionality, each microstructural feature has associated with it, size, shape, volume, surface area, curvature, etc., and location. Therefore, a microstructure can be quantitatively characterized via estimation of important attributes of these geometric features and their spatial arrangements. Numerous stereological relationships are available for unbiased and assumption estimation of the attributes such as volume fraction [DeHoff and Rhines, 1968; Underwood, 1970], surface area[Smith and Guttman, 1953; Baddeley et al., 1986; Gokhale and Drury, 1994], total length[Gokhale, 1990 and 1992], curvature[DeHoff, 1967; Cahn, 1967; Gokhale,1998], average volume, and size and orientation distribution of the microstructural features[Saltykov, 1958; Cruz Orive, 1976; DeHoff, 1962; Gokhale, 1996; Benes et al., 1997] from the measurement performed on random (or design based) two dimensional sections or projections through the three-dimensional microstructural space. Distribution of relative locations of microstructural features is manifested in spatial patterns, pair correlations, n-point correlations, clustering, short and long range interactions, etc. The spatial arrangement of features (such as pores, grains, particles, et.) in microstructure is reflected in particle packing, connectivity, distribution of inter-particle contacts, percolation thresholds for rigidity, etc. The spatial arrangements of pores and grains in the concrete microstructure are expected to affect the properties of the concrete and the damage evolution in the concrete. However, to the best of our knowledge, there are no experimental data whatsoever on first, second, and higher order nearest neighbor distributions, or on any other measures of spatial arrangement of features in three-dimensional opaque microstructure of concrete. This is primarily due to lack of suitable experimental techniques for estimation of descriptors of spatial arrangement of features in three-dimensional microstructure. Recently, Gokhale and co-workers have developed digital image analysis techniques for reconstruction of a large volume of three-dimensional microstructure at high resolution from large area high resolution montage serial sections[Gokhale, et al., 1998; Tewari et al., in press; Tewari, 1999; Tewari and Gokhale, in press]. The technique has been utilized for quantitative characterization of spatial arrangement of features and other attributes of three-dimensional microstructure of a liquid phase sintered W-Ni-Fe alloy that is widely used for making ammunition projectiles. In the Phase-II of this SBIR, we propose to modify and extend these digital image analysis based methods for quantitative characterization of three-dimensional microstructure of concrete and associated microstructural damage. These unique experimental data will provide new insights into microstructure–properties relationships in granular materials like concrete as well as damage evolution (micro-cracking) etc. in these materials. The image analysis base methodology is described below.

Let us consider characterization of spatial arrangement of features in three-dimensional microstructure (of say concrete), which obviously involves measurement of inter-feature distances in three-dimensional space. For opaque materials, a segment of three-dimensional microstructural volume can be reconstructed from a stack of serial sections. In the conventional serial sectioning [Rhines and Craig, 1976; Liu et al., 1994], one microstructural field of view on a metallographic plane is recorded (digitally or in a photo-micrograph), the specimen is polished to remove a small thickness of material, and then microstructural field in the second metallographic plane in exactly the same region is recorded again. This polish - record image of field of view - polish procedure is repeated to generate a large number of serial sections (typically 50 to 100). The three-dimensional microstructural volume segment can be then reconstructed from such a stack of well aligned serial sections. This conventional serial sectioning technique is very inefficient, because it involves a lot of effort to generate only a small high resolution segment of three-dimensional microstructure. The cross-sectional area of this field of view is equal to the area of one microstructural field observed in a metallographic plane. This 3D reconstruction leads to serious practical difficulties[1]: for example, measuring distance between two features present in Figure 3.2.5 as a nearest neighbor distance would be completely wrong, because nearest neighbors of these features are in the adjoining volume segments (Figure 3.2.6) which have not been reconstructed. This bias is higher and higher for second, third, and higher order nearest neighbor distances. Further, from such small volume segment, it is obviously not possible to get any information about spatial arrangement of features at distances larger than about one third of the size of the volume element. Therefore, it may be concluded that the conventional serial sectioning is time consuming and inefficient, and it generates a small segment of three-dimensional microstructure which is not useful for quantitative characterization of spatial arrangement of features in three-dimensions.

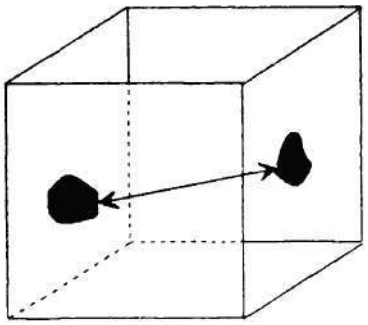

Figure 3.2.5. A 3-D cubic element of the microstructure showing two pores. Analogous to Figure 3.2.5, on observing just this element one may reach to a wrong conclusion that these two pores are the nearest neighbor of each other.

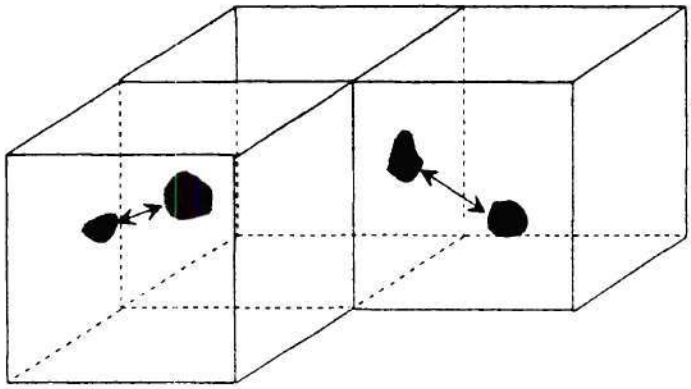

Figure 3.2.6 A 3-D analog of montage is shown with three cubic elements of the microstructure with the center element being the same as in Figure 3.2.5. It is now clear that the nearest neighbors of the two pores in the center element are present in the adjoining cubes. Thus the conclusions about nearest neighbor cannot be drawn from observations of just one isolated cubic element.

To generate a large volume of three-dimensional microstructure at high resolution, one may first reconstruct many contiguous small volumes surrounding the one shown in Figure 3.2.5, and then perfectly match their boundaries and paste them together to generate a large volume of three-dimensional microstructure. If the volume of the recreated microstructure is sufficiently large then it can eliminate the "edge effects" for all practical purposes. Using such a high-resolution large microstructural volume, one can then precisely measure distances between two features located any where in such a three-dimensional "montage". Gokhale and coworker[Louis and Gokhale, 1995, 1996; Yang et al., 1996, 1997; Tewari et al., 1998; Dighe et al., in press] have developed a method that is equivalent to such a reconstruction. First a "montage" of a large number of contiguous microstructural fields (say 25 to 100) observed in a metallographic plane is created. The procedure involves grabbing overlapping contiguous microstructural fields by using an image analyzer, and then boundaries of the contiguous microstructural frames are perfectly matched (within one pixel) by using interactive image analysis to generate a large area high resolution 2D microstructural "montage" [Gokhale et al., 1998; Tewari et al., in press; Tewari, 1999]. This is followed by removal of small thickness of material (about one micron) by polishing and then a second montage is created at exactly the same region in the second metallographic plane. This polish-montage-polish procedure is repeated to obtain a stack of 75 to 100 montage serial sections. The montage serial sections are then precisely aligned in the Z-direction by using image processing techniques, the details of which are described in a subsequent section. The effort involved in this process of creating a stack of montage serial sections is comparable that for the conventional serial sectioning, but the montage microstructural volume is 25

to 100 times larger than that generated by conventional serial sectioning. Therefore, such a high resolution large volume can be used to quantitatively characterize short range, intermediate range, and long range spatial arrangement of features in three-dimensions with high precision. Further, the use of montage leads to a very efficient serial sectioning technique as it can yield 25 to 100 times larger sample of three-dimensional microstructure than that obtained by conventional serial sectioning with the same effort. The details of this technique are described below through an application involving three-dimensional reconstruction of W grains in a liquid phase sintered W-Fe-Ni alloy.

Experiments were performed on a liquid phase sintered 83wt% W-Ni -Fe alloy. The specimen was mounted and polished with diamond polishing medium using standard techniques. For digital image analysis, it was necessary to develop a microstructure with good contrast between W grains and the matrix. This was achieved by using interface layering technique developed at NASA Lewis Research Center. The sample was coated with a thin layer of platinum oxide (PtO) by sputtering platinum on the sample kept in oxygen atmosphere. Figure 3.2.7 illustrates microstructure revealed in this manner.

Microstructure in Figure 3.2.7 reveals that although average size of W grains is on the order of 11 μm, the separation distance between many grains is on the order of few microns. Therefore, if this microstructure is observed at a low magnification, many closely spaced W grain sections will not be resolved as separate individual grain sections (as in Figure 3.2.7b), which can lead to erroneous results. Therefore, for sufficient resolution, the digital image analysis has to be performed on microstructural images observed at a sufficiently high magnification (in this study, 500X). However, at such high magnification, only a very small region of microstructure is observed , and typically, each field of view contains only 30 to 40 W grains (see Figure 3.2.7a), and the nearest neighbors (particularly, second and higher order neighbors) of numerous of grains are not likely to be present in the same field of view. Therefore, there is a need to create a high resolution large area montage, to characterize spatial arrangement of W grains.

A. Creation of Microstructural Montage

In this work the image analysis was done on KS-400 image analysis system from Kontron, Inc. However, several other commercial image analysis systems also have the required capabilities. The computer codes for creating the montage were written in a language similar to C in a platform provided by the image analysis software (KS-400). To create the montage, the first field of view (FOV) was arbitrarily chosen and the image of this field of view was then stored in the memory of image analysis computer as an image file. The right border (of about 60 pixel width) of this image was recalled on the left edge of a blank image. This semi blank image was then displayed along with the live image. This resulted in a superimposed image on the left border of the screen (of the previous right border and live image) with rest of the screen having the live image (see Figure 3.2.8). The computer controlled microscope stage was then automatically moved so that the right border of the live image moves to the left border

and gives a reasonable match with the superimposed image. The physical movement of the automatic-stage has a large least count and thus cannot achieve perfect match with the previous image, thus small movements (to a least count of one pixel) of the live image were made manually using image analyzer to achieve a perfect match. This resulted in a match of the first and the second image with an accuracy of one pixel. This second image was then stored in the computer memory as another image file. All successive images were grabbed by using the same procedure and finally a continuous montage of fields was made. The details of montage creation are described elsewhere [Tewari, 1999; Tewari and Gokhale, in press]. Figure 3.2.9(a) shows a montage of twenty-five fields of view, which has been compressed for display. Each region of this montage has a high resolution of the image shown in Figure 3.2.9(b). Therefore, montage is a microstructural image of a large area (twenty-five fields of view at 500X) having high resolution.

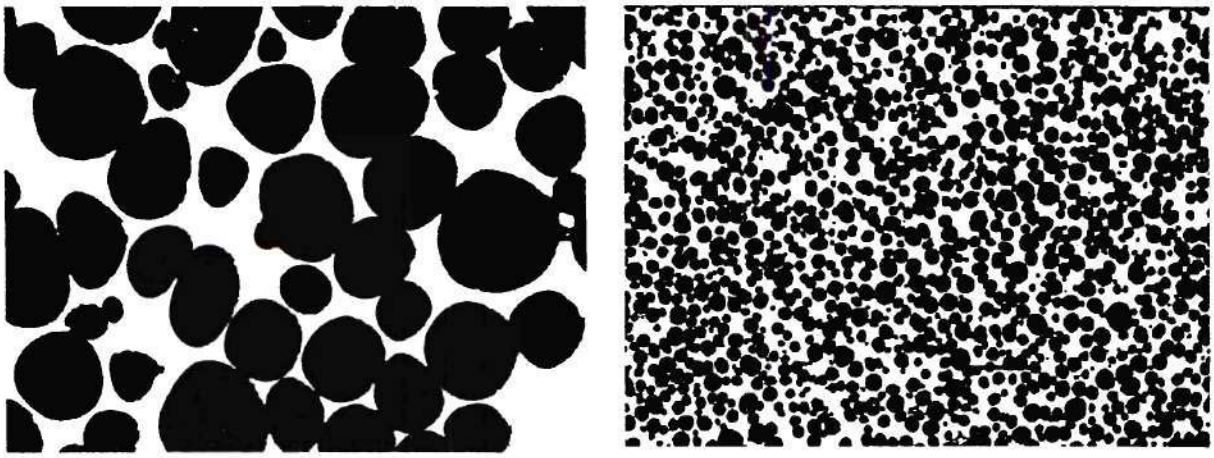

Figure3.2.7 a) A typical micrograph of 83 wt% W 11.9% Ni and 5.1% Fe alloy liquid phase sintered in microgravity at 1780 K for a duration of 1 minute. b) A low resolution micrograph of the same alloy as

Figure 3.2.8 A display frame in the process of montage creation. The frame shows a live image with a superimposed image on the left border (the superimposed image is made up of the live image and the right border of the previous image).

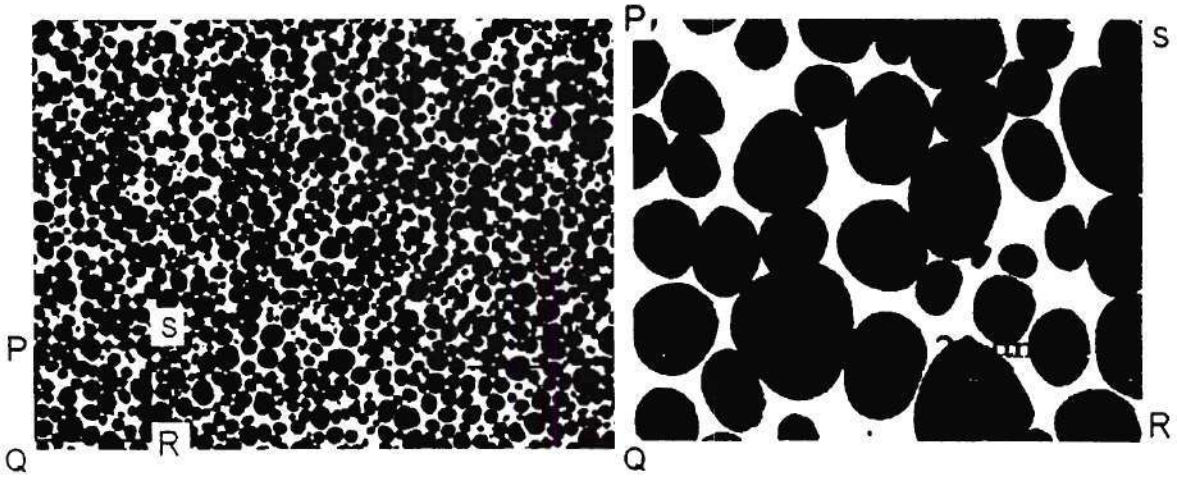

Figure 3.2.9 (a) A montage of twenty-five microstructural fields, which is digitally compressed for display, (b) Each field of view (say PQRS) in the montage (a) has the same resolution as that of the field shown here.

B.Generation of Montage Serial Sections

A rectangular region of interest was chosen on the metallographic section to make a montage of twenty-five (5X5) microstructural fields. Four diamond micro-hardness indents were made on the selected region, one at each corner. These indents were made to measure the thickness of material removed in successive serial sections (explained later) and to provide reference points to get back to exactly the same region of the microstructure in successive serial sections. A fixture was molded on the microscope stage which had a hole at the center to hold the sample. The fixture was so molded that it could hold the sample in only one specific orientation, thereby keeping successive serial sections aligned within about five degrees. After making the indents, a montage of the region was digitally grabbed (as described in the previous section) and labeled as section 1, and saved in the hard drive of a computer. The sample was then polished to remove of a thin layer (1 to 2 μm) of the sample. The sample was then cleaned, dried and coated with PtO to develop contrast between the tungsten grains and Ni-Fe-W matrix by interface layering. The sample was then again taken to micro-hardness tester and new indents were made beside the old indents (which had grown small in size because of sectioning). After making the new indents, the sample was placed in the fixture on the microscope stage and the stage was moved till the first corner of the

rectangular region was seen through the microscope. The image of this FOV was superimposed on the image of the same region taken before sectioning (from image of section 1 stored in the hard drive). The micro-hardness indents were seen on the superimposed image and the microscope stage was moved till the indents on the two image were matched. This insured that the location being viewed in the microscope is the same as in the previous serial section. After alignment, another montage of twenty-five microstructural fields was grabbed, and stored in the hard-drive as an image labeled section 2. By repeating the above process of polishing, coating, indenting and grabbing one can record as many serial sections as one wants and recreate the volume. Figure 3.2.10 shows few montage serial sections stacked on top of each other.

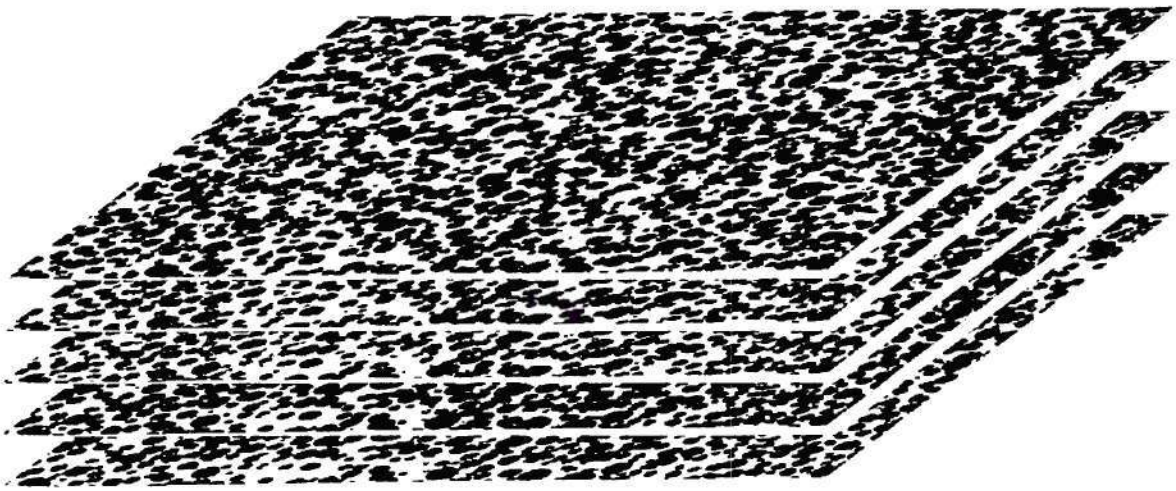

Figure 3.2.10 Stack of serial sections. Ninety such serial sections were used for 3-D reconstruction.

C. Measurement of Distance Between Successive Montage Serial Sections

To be able to perform any quantitative measurements on the volume generated by serial sectioning, one needs to know the exact amount of material removed between consecutive serial sections, so that the depth dimension of the grains can be quantified. The thickness of material removed between two consecutive serial sections was calculated by measuring the size of the micro-hardness indents. The indents were made by a square

pyramidal shaped diamond with opposite faces at an angle of 136 degrees. This means that the ratio of the diagonal of the square formed on the section to the depth of the indent is 2%2tan(136E) which is equal to 7.00. Thus for a unit change in diagonal length there was 1/7 change in the depth. The change in the diagonal was measured using digital image analysis for each section at each corner and mean value was taken and was used to calculate the change in indent depth, and thus the distance between consecutive serial sections. Figure 3.2.11 shows two images with micro-hardness indents. It can be seen that as the material is removed the indents become smaller in size, and these indent size data can be used to measure distance between consecutive serial sections.

D. Alignment of Serial Sections

An important problem in serial sectioning is that the consecutive sections are usually not aligned; they have some transnational and rotational displacement with respect to each other. In the present study, in spite of adjusting the microscope stage, the serial sections grabbed were not perfectly aligned, but were displaced by up to ten pixels at the most by about five degrees, and therefore it was essential to perfectly align them. Alignment can be done by locating two common points in two consecutive serial sections and translating one image till the first common point is aligned in the two images. Then the image is rotated about this point till the second common point is also aligned. This was done by using 3D image analysis software Voxblast 3.10 in which the images of the montage were digitally translated and rotated till they were exactly aligned to the respective previous sections.

E. Visualization of Three-Dimensional Microstructural Volume

Volume image data have been used for visualization of numerous structures and processes in three-dimensions. Sources of volume data differ in modalities. X-ray computed tomography(X-ray CT), single photon emission computed tomography (SPECT), positron emission tomography (PET), magnetic resonance imaging (MRI), serial sections, and ultrasound imaging are some of the most common modalities. The volume image data presented in this research are stack of montage serial sections. The steps required to visualize these data are: data generation (stack of serial sections), pre-processing (image alignment and correction, grid regularization, image enhancement and interpolation), data classification, and finally rendering. The microstructural volume visualization can be done by either surface rendering or volume rendering. Surface rendering is defined as rendering of iso-surface of the region of interest (ROI) from the volume data, whereas volume rendering is the rendering of all the volume data by specifying color and opacity of each voxel (which is analogous to pixel in two dimensional digital image). The

advantage of surface rendering is that it results in reduction of data (only surface data is retained) and is easy the understand, but has a disadvantage that lot of volume data are discarded and thus one needs to extract iso-surface data every time one changes ROI.

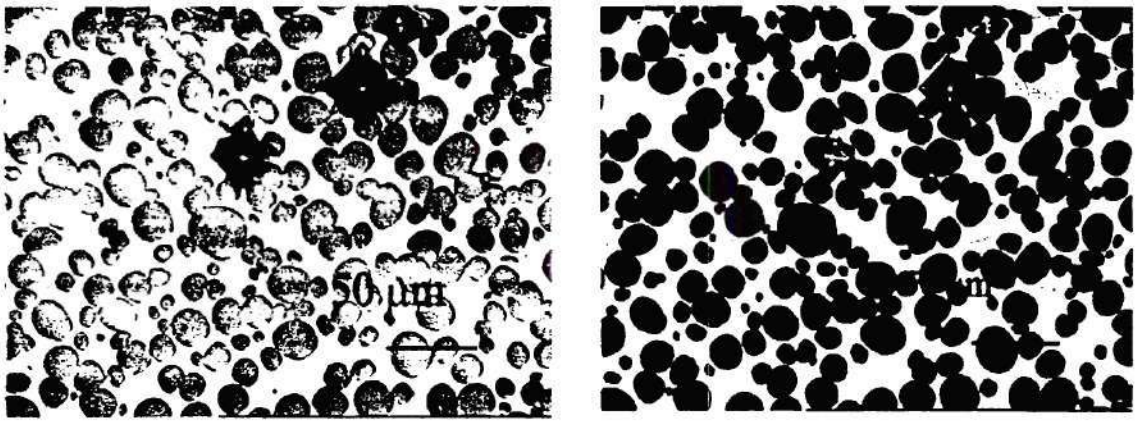

Figure 3.2.11 Two micrographs showing the fading micro-hardness indents on the metallographic sections on serial sectioning. These indents were used for measuring the amount of material removed during each sectioning and for aligning the serial sections.

The data classification step for surface rendering requires fitting of a surface in the volume data. The basic idea in data classification is to look for one surface to visualize, identify the intensity corresponding to that surface and threshold the selection. One of the oldest surface rendering algorithm is contour connecting algorithm [Sabella, 1988; Keppel, 1975; Lorensen and Cline, 1987]. In this algorithm iso-contours are thresholded and extracted in each slice (serial section), then contours between adjacent slices are connected and then rendered. The main deficiency of this algorithm is the problem in connecting contours between adjacent sections . The algorithm used in this research to extract iso-surfaces is known as marching cubes algorithm[Lorensen and Cline, 1987]. In this algorithm cell representation of the volume data is taken. Each data sample in the cell (i.e. each vertices of the cell) is considered either inside the surface of interest or outside depending on whether it is above or below the threshold value. For a cubic cell there are 256 (because there are 8 cube vertices => 2^8 =256) possible above/below threshold combinations, but only 15 unique (canonical) cases are possible. For each of these case, one can interpolate the surface intersection along the edge and generate surfaces and surface normals. These iso-surfaces can then be used for surface rendering. In the process of volume rendering, all voxels are visualized by specifying a mapping between rendered image intensity and voxel intensity. In this study, Ray-Casting algorithm was used for volume rendering [Sabella, 1988; Keppel, 1975; Lorensen and Cline, 1987]. The basic idea of this algorithm is

to cast a ray from the eye through the image plane and collect color and opacity at intersected voxels . Because the data traversal in this algorithm is from the image plane to the volume, it is also known as image order algorithm. Along each ray cast from the eye, the field is expressed as a function of the ray parameter. The algorithm computes properties of the field along the ray such as the attenuated intensity, the peak density, and the center of gravity, etc. These are mapped into HSV color space to produce an image for visualization. Images produced in this manner are perceived as a varying density 'cloud' where intensity highlights the computed attributes.

F. Reconstructed Three-Dimensional Microstructures

Figures 3.2.12 and 3.2.13 show volume rendered and surface rendered three-dimensional microstructure of tungsten grains in the liquid phase sintered 83wt% W-Ni-Fe alloy obtained by this technique. Note that the three-dimensional microstructures shown in these figures is only about 5% of the total microstructural volume contained in the stack of montage serial sections. The surface rendered microstructure (Figure 3.2.14) is equivalent to the one that would result if matrix is etched away from the microstructure. Figure 3.2.14 reveals that the structure has very high degree of topological connectivity; almost all W grains are interconnected.

G Quantitative Data on Spatial Arrangement of Grains in Three-Dimensions

The frequency function of the distribution of inter-particle contacts and average number of inter-particle contacts per grain are very important microstructural parameters in the theories and models for liquid phase sintering. Figure 3.2.14 shows the three-dimensional first, second, and third nearest neighbor distribution function of W grains in the present liquid phase sintered specimen, and the corresponding mean near neighbor distances. To the best of our knowledge, these three-dimensional distributions have never been experimentally measured; this is the first set of such experimental data on material microstructures. Figure 3.2.15 shows the experimentally measured frequency function of number of inter-particle contacts between W grains in three-dimensional microstructure estimated from the present data. In this specimen, average number of inter-particle contacts per grain is equal to 3.05, although volume fraction of W grains is 0.59. Note that for a simple cubic arrangement of mono-sized spheres, number of inter-particle contacts is equal to six at particulate volume fraction of 0.52.

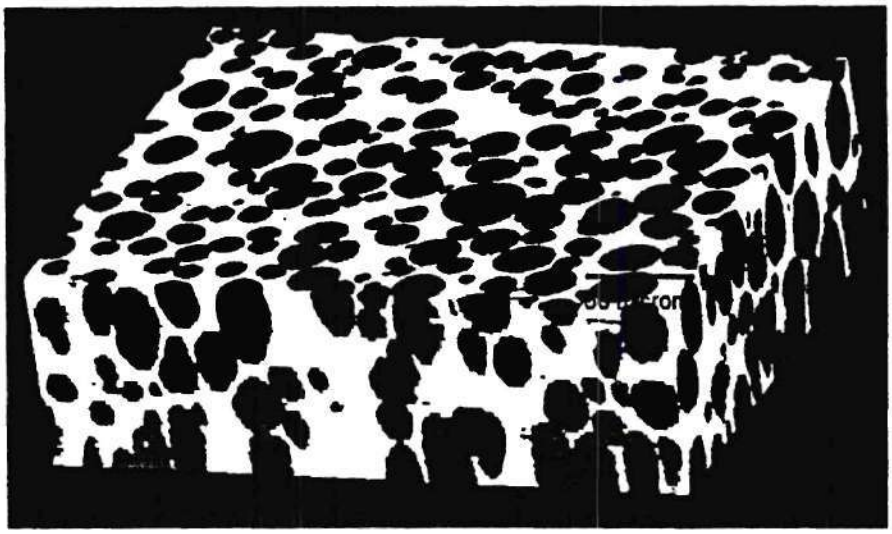

Figure 3.2.12 A volume rendering of the 3-D microstructure reconstructed from serial sections.

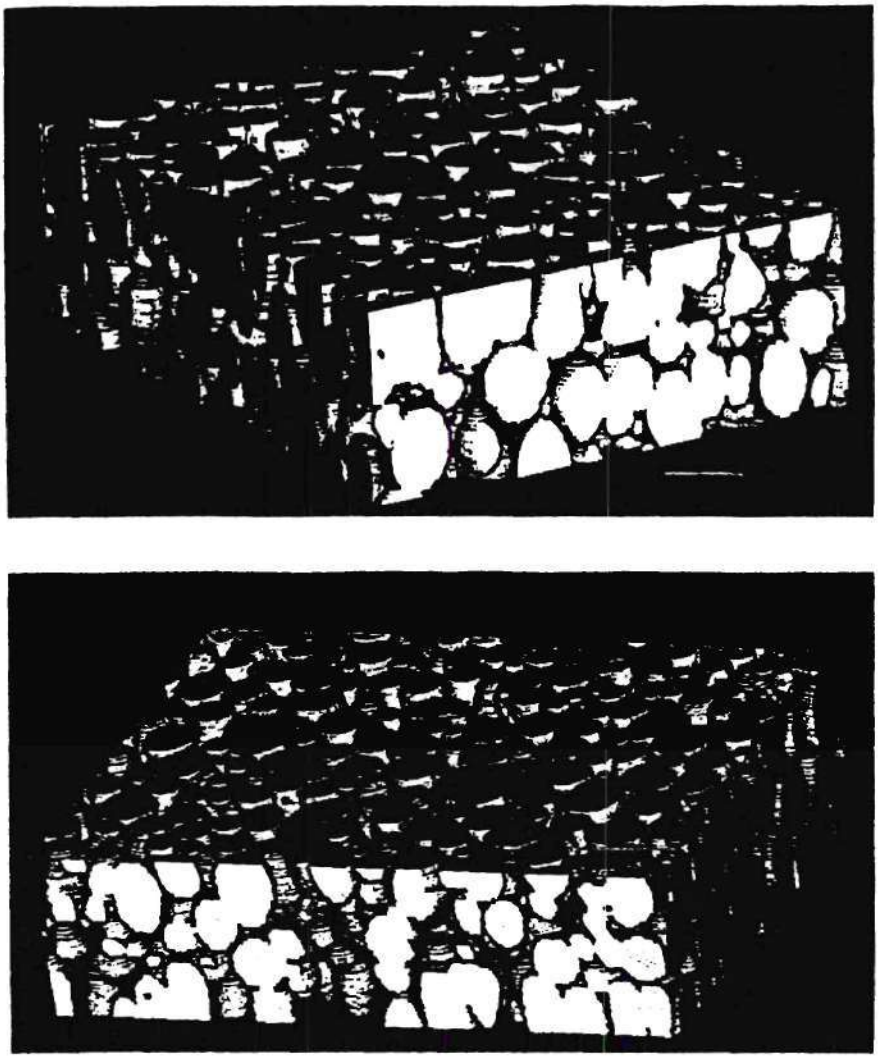

Figure 3.2.13 Two views of surface rendered 3-D microstructure reconstructed from serial sections.

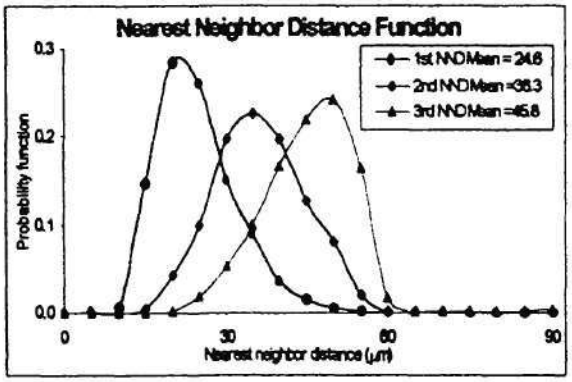

Figure 3.2.14 First, second and third nearest neighbor distribution function for the tungsten grains.

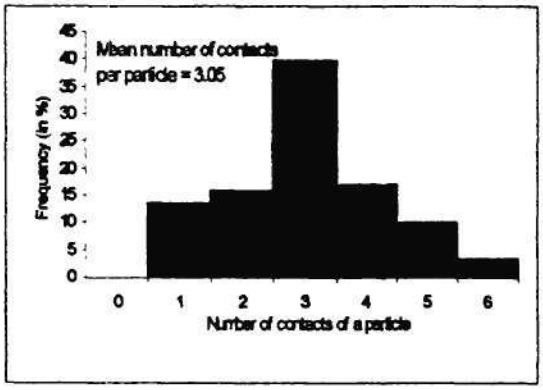

Figure 3.2.15 Distribution of number of contacts per particle in 3D.

C. Task 3: Identification of Microstructural Damage Quantities

Shrinkage and Crack Initiation:

In Portland cement concrete, both the cement paste and the aggregate phases are brittle, and each phase approximately obeys Griffith crack theory. The process of crack initiation before a specimen is subjected to loading is important in characterizing the fracture characteristics of the concrete. Cracks may occur predominantly in the continuous phase (paste or mortar), the disperse phase (aggregates), or at the interface. The crack locations depend on relative elastic moduli, Poisson's ratios, and the strengths of the paste and the aggregates. Other factors that can also affect the crack location include size, shape and surface texture of the aggregate particles, and the fresh (plastic) properties of cement paste in the concrete.

In concrete, crack initiation before loading results primarily from shrinkage strains in the cement paste, and/or at the paste/aggregate interfaces. Shrinkage results from the loss of water from cement gel and increases with the amount of water used in the concrete mix. The introduction of sand and coarse aggregate into the cement paste reduces the drying shrinkage by (1) reducing the amount of dimensionally unstable component, (2) producing a restraint effect which reduces volume change. On the other hand, introducing coarse aggregates into the cement paste creates the interface between these two phases, and crack initiation can occur at the interface due to the restraint effect of the coarse aggregate particles. This is particularly critical for concrete containing large coarse aggregate particles. Large aggregate particles also have the tendency to trap the water segregating from the cement paste at the underside of the aggregate particles, creating a weak interfacial transition zone (ITZ). It has generally been observed that the bond between coarse aggregate and mortar is the weakest link in a heterogeneous concrete system.

In conjunction with the drying shrinkage there is thermal strain induced in the paste and at the interface as the results of non-uniform thermal gradients developed in the concrete due to rapid temperature changes. This latter scenario often contributes to the cracks developed in prestressed concrete beams when the steel form is demolded in the casting plant. A sudden drop in the concrete temperature on the surface of the beam while the concrete in the interior of the beam remains warm creates sufficient tensile strain on the concrete surface to cause the crack to initiate on the surface.

Loading and Crack Propagation

Crack propagation during loading may occur at the aggregate-paste interface, in the paste or mortar matrix, or in the aggregate particles. Crack propagation during loading can be detected by a reduction in the slope of the stress-strain curve (elastic modulus), by an increase in the Poisson's ratio, by direct microscopic observation or imaging technique on the specimen surface, or by a reduction in the velocity of acoustic or other waves through the

specimens. Crack geometries and distributions on sections cut after loading have already been studied using imaging techniques [Malvern, et al, 1992; Nemati et al., 1995].

In ideal brittle materials, when a crack reaches critical size, it propagates spontaneously through the material. In a heterogeneous material, such as concrete, the crack is initiated from the weak component, such as the interface transition zone (ITZ), it may extend into a zone of increased resistance, stop, and then extend again at a higher stress level, resulting in non-linearity in the stress-strain curve. In contrast, the stress-strain relationship of pure cement paste is, for example, linear up to failure.

Based on quasi-static tests, several stages of cracking under loading can be distinguished. These are:

- Crack initiation. Upon initial loading up about 40% of the ultimate strength, additional microscopic cracks appears at points of high tensile strain concentration.
- Stable crack propagation. As load is increased from 40% to about 70%, cracks propagate.
- Unstable crack propagation. When the applied load exceeds 70% to 90% range cracks become self-propagating under constant applied load, and failure occurs whether or not load increases.

Relationship of Microstructural Damage to Material Properties

As discussed above, in addition to the properties of the constituent materials, the characteristics of micro-cracks and the aggregate/paste interface transition zone can have a significant effect on the macro-scale properties of concrete. The influence of micro-crack density and other micro-defects on concrete properties has been investigated extensively. These include correlating elastic and bulk modulus with crack density (Budiansky and O'Connell, 1976), elastic modulus and compressive strength with void and pore distribution (Zhang, 1998), fracture toughness and fractal properties of rough surfaces (Abell and Lange, 1998), strain energy with branching dimensions (Nakasa et al., 1994), crack to micro-crack interactions with energy release rate (Chudnovsky and Wu, 1990). These relations are either derived from micromechanics with an assumed size and distribution of micro-cracks or through experimental observations. With the micro-mechanics derivations, micro-crack interactions are usually not adequately accounted for. In the experimental correlation studies, only limited tests have been performed. No reliable experimental validation of these relations has been pursued for lack of coordinated efforts and consensus microstructure parameters.

The important macro-properties of concrete include compressive and tensile strengths, elastic modulus and bulk modulus, toughness and plastic deformation properties. Tensile strength and toughness are considered to be the most important properties under projectile penetration loading conditions. Both crack initiation and propagation are controlled by the toughness of aggregates, paste and ITZ. The compressive strength is actually controlled by

the internal tensile stress of concrete. The important parameters of microstructure damage parameters for concrete include specific crack surface tensor, local volumetric fraction of voids, paste and aggregates, density of interfacial transition zone, mean free path, clustering, branching, fractal surface of voids and cracks, and bivariate void distribution. Among the microstructure damage parameters listed above, not every one of them has equal importance in its effect on different macro concrete properties. Quantification of various microstructure quantities may be conveniently implemented if high-quality images and automatic data reduction system can be developed. As many of the microstructure quantities can be quantified quite conveniently by the procedures we developed, a multiple-factor correlation method can be used for correlation analysis, which has not been achieved as a result of the lack of reliable quantification methods to date.

Microdamage Quantities Identified

The microdamage quantities that have significant influence on macro concrete properties have been identified through literature review and Phase I study. These quantities include:

1. Specific Cracked Surface Area: an overall indication of the damage status, its tensor format is directly associated with damage tensor used in continuum damage mechanics (CDM) to estimate effective moduli, strength and toughness.

2. Mean Free Path: the average spacing among cracks, it is an indication of the cracking interaction effects.

3. Bivariate Distribution of Crack Size and Orientation: this quantity can be directly used in micromechnics and continuum damage mechanics (CDM) to estimate effective moduli, strength and toughness.

4. Branching Effect: related to material toughness and strain rate effects.

5. Density of Interfacial Transition Zone: a weak zone between aggregates and paste, cracks often initiated from this zone and propagate through this zone.

6. Void Size Distribution and Spacing Factor: these quantities affect the freeze-thaw resistance, they are also important in the crack propagation process.

7. Fractal Characteristics of Crack Path and Fractured Surface: the rough surfaces will affect the fracture toughness calculation.

8. Local Volume Fractions (LVF) of Different Phases: as noticed in the penetration tests, the plastic deformation at the crater and around the projectile-concrete interface is very significant, indicating distortion and compression of different phases. LVF can represent the plastic deformation effects.

D. TASK 4: DEVELOPMENT OF DATA REDUCTION SOFTWARE

The microdamage quantities are geometric quantities, the quantification methods developed for one quantity may be applied to another quantity. For example, the method developed for quantifying cracked surface area can be used to quantify other surface areas such as the ITZ, void and aggregate as long as the sample size is statistically sufficient. The members of the research team have accumulated more than 20 years experience in sample preparations, quantification methods and computer software development in image analysis and have more than 100 published papers in this area. Software developed by the research team for various micro-damage quantities is listed below. A specific sampling scheme has also been developed for each of the methods. For example, quantification of the three-dimensional cracked surface area tensor requires images from three orthogonal surfaces, the fractal analysis requires the feature images at different scales. The computer programs include our previous developments and new developments. It is convenient to assemble these programs into an independent software package for image acquisition, processing, microstructure quantification, effective property evaluation and numerical simulation. The team is confident of achieving this objective as most of the developed procedures have already been successfully adapted to the use in the concrete project.

As most of these developed programs have been developed by the team members for the applications to other materials such as soil and metal. Detailed explanations on the algorithms have been addressed in corresponding references and will not repeated in this report for conciseness.

Table 4.1 A List of the Computer Programs Developed by the Research Team

Program Name	Functions	Relevant Publications
SurfQuant	Quantification of surface area, cracked surface area density, interfacial transition zone, fractured surface	Frost & Kuo (1994)
MeanFreePath	Quantification of the average spacing between cracks, voids and other features to indicate interactions among different components	Frost & Kuo (1998)
LocalVolume Fraction	Quantification of the local volumetric fractions of different components of a heterogenous material such as concrete	Frost & Kuo (1996)
Trisector	Quantification of the bivariate size and orientation distribution of cracks, characterization of fractured surfaces	Gokahale (1996)
Connectivity	Characterization of the connectivity or percolation of cracks, and other components	Gokhale (1996)
Kinematics	Characterization of particle rotation and translation, strains in the mastic and at interfaces	Frost & Wang (1999)
FourierFractal	Implementation of Fourier and fractal analysis of curves	Frost & Wang (1997)
Branching Clustering	Analysis of the branching and clustering effects of cracks and voids	In development.

E. TASK 5: ILLUSTRATION OF THE USE OF THE DEVELOPED TECHNIQUES

Specific Quantitative Microstructure Measurements

As part of Phase I tasks, images captured from coupons cut from an actual tested target are being evaluated. These images are being evaluated using a variety of algorithms developed/adapted for this project by the team members. These include algorithms to determine parameters such as local void ratio distribution, mean free path, surface area, volume fraction of various phases, various void and particle tensors. Example determinations by applying the algorithms to images captured from a dissected target specimen are illustrated in the following figures.

Figure 3.5.1 presented a set of four images acquired at locations at different distances away from the tunnel. The phenomena to emphasize are that cracks in the aggregates are parallel to the radial direction. These cracks are believed to be generated by the circumference tensile stress resulted from the radial compression stress. It should be also noted that aggregates closer to the tunnel are more severely cracked.

Figure 3.5.2 presented a gray image and its binary images corresponding to voids and aggregates for illustrating the quantification of volume fractions, specific damaged surface area (ITZ, void surface area), and mean free path among different constituents. The corresponding tensors will be determined using a separate example. As was discussed in detail in the previous sections, the determination of the statistically meaningful quantities needs the use of image montage.

Figure 3.5.3 illustrated an example for determining the fractal dimension of ITZ. Similar procedures can be used for the determination of the fractal dimension of cracks and void surfaces.

Figure 3.5.4 illustrated an example for the quantification of nearest neighbor distance and interaction factor of voids in two dimensional sections. In the Phase II study, a comparison of the quantities determined from 2D sections and 3D volumes shall be made. It should be noted that 2D determination only provides inaccurate index values.

Figure 3.5.5 illustrated the phenomenon of crack branching and the necessity of the study of the projectile-concrete interface properties.

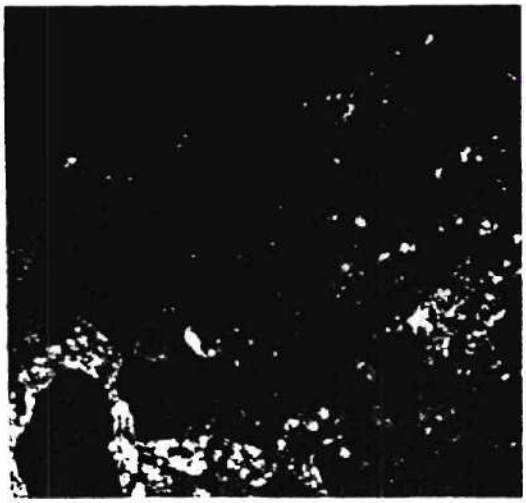

(a) Crack Path and Void Locations (Magnification 10 – Approx. 3.5" from Tunnel Edge)

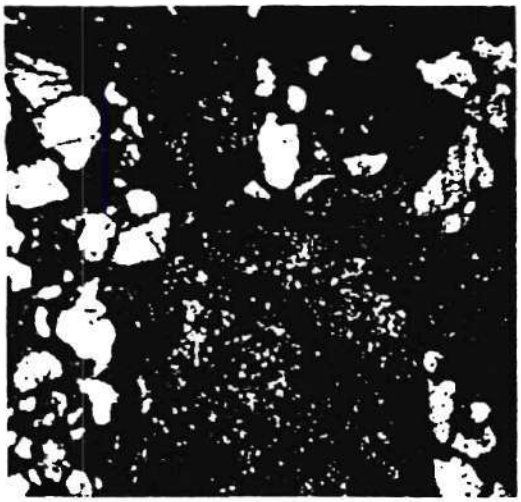

(b) Crack Penetrating into Aggregates (Magnification 40 – Approx. 2.5 " from Tunnel Edge)

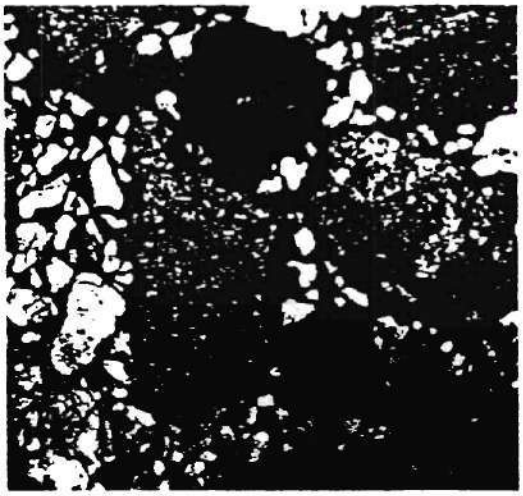

(c) Aggregate Crushing and Voids (Magnification 20 – Approx. 1.5" from Tunnel Edge)

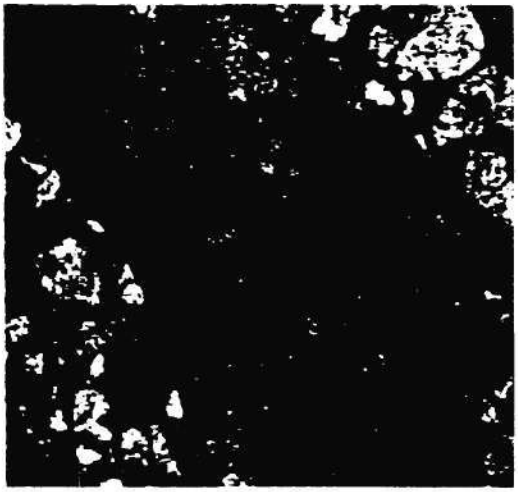

(d) Aggregate Crushing Closer to Tunnel (Magnification 40- Approx. 0.5" from Tunnel Edge)

Figure 5.1 Example Images Showing Crack Propagation and Aggregate

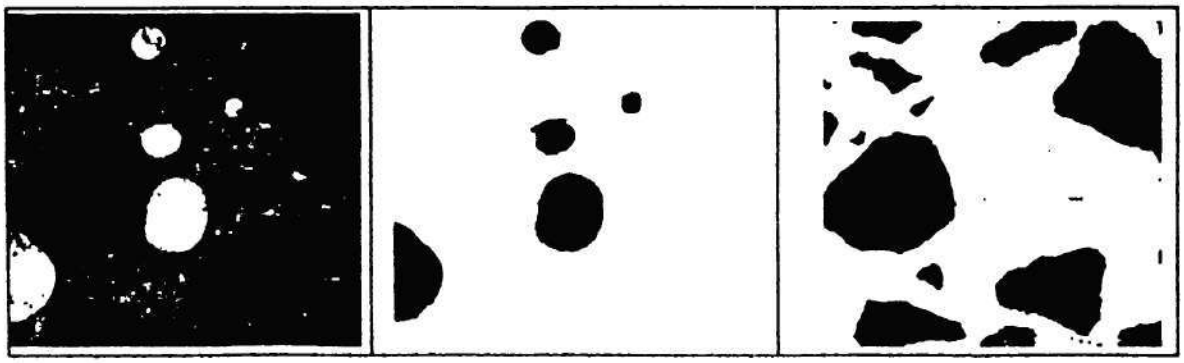

Gray Image Voids Aggregates and ITZ

Figure 3.5.2 Images for Example Determination of Volume Fraction, SSA and MFP

Table 5.1 Microstructure Quantities Determined

Quantities	Voids	Aggregate	Mortar
Area Ratio	8%	32.1%	59.9%
Specific Surface Area (SSA)	0.007/piexl	0.025/piex	NA
Mean Free Path	361 pixel	96.4 pixel	NA

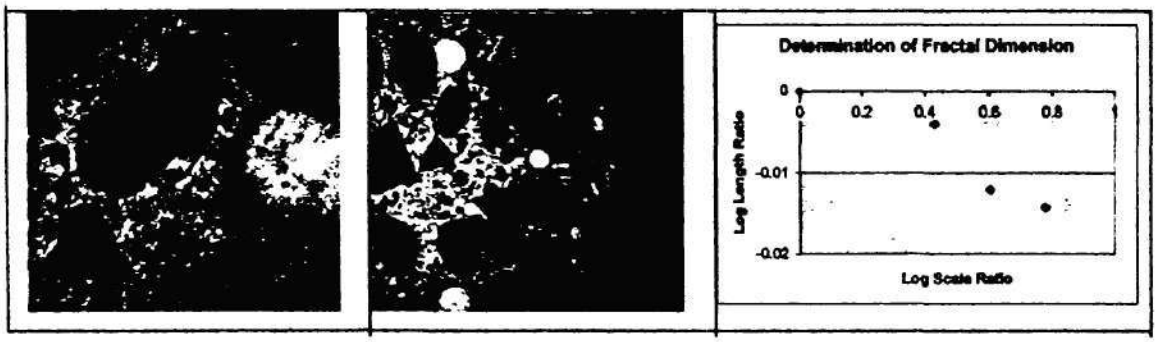

Figure 3.5.3 Characterization of Fractal Nature of ITZ, Crack Path and Fractured Surface (example, ITZ)

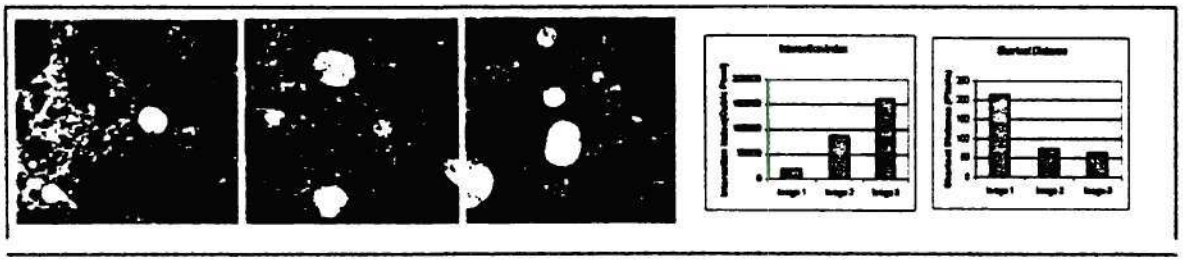

Figure 3.5.4 Quantification of Nearest Neighbor Distance and Interaction Factor of Voids

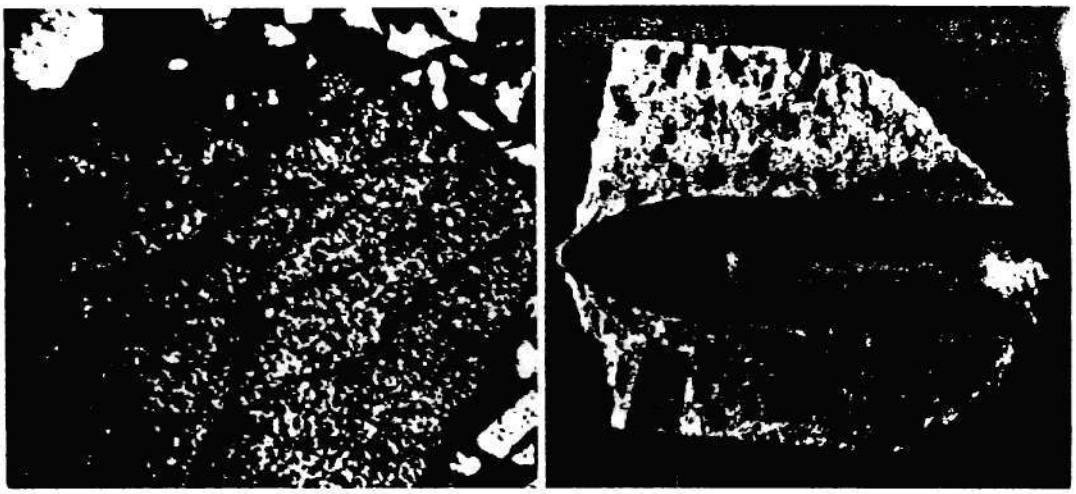

Figure 3.5.5 Characterization of Crack Branching and Projectile-Concrete Properties

Figure 3.5.6 Illustrated the variation of the cracked area (volume) and pseudo-damaged surface area along the radial direction as a function of distance from the tunnel. The determinations are performed on the image montage presented in Figures 3.2.2 and 3.2.3. The pseudo-damaged surface area is actually the perimeters of the cracks on a 2D section, it is related to the 3D surfaces by average curvatures in the direction of the normal to the section.

Figure 3.5.7 is an example determination of the mean solid path and mean solid path tensor at two different locations where crack patterns are significantly different. The results indicated the rationality of these numbers.

Figures 3.5.8 is an example determination of the mean solid path and mean solid path tensor, the specific damaged surface area and the specific damaged surface area tensor in 3D. Theoretically the three images (or three image montages) should be from three orthogonal planes, however, in this example the three images were actually from one section. In the actual quantification of these quantities, image montages must be used.

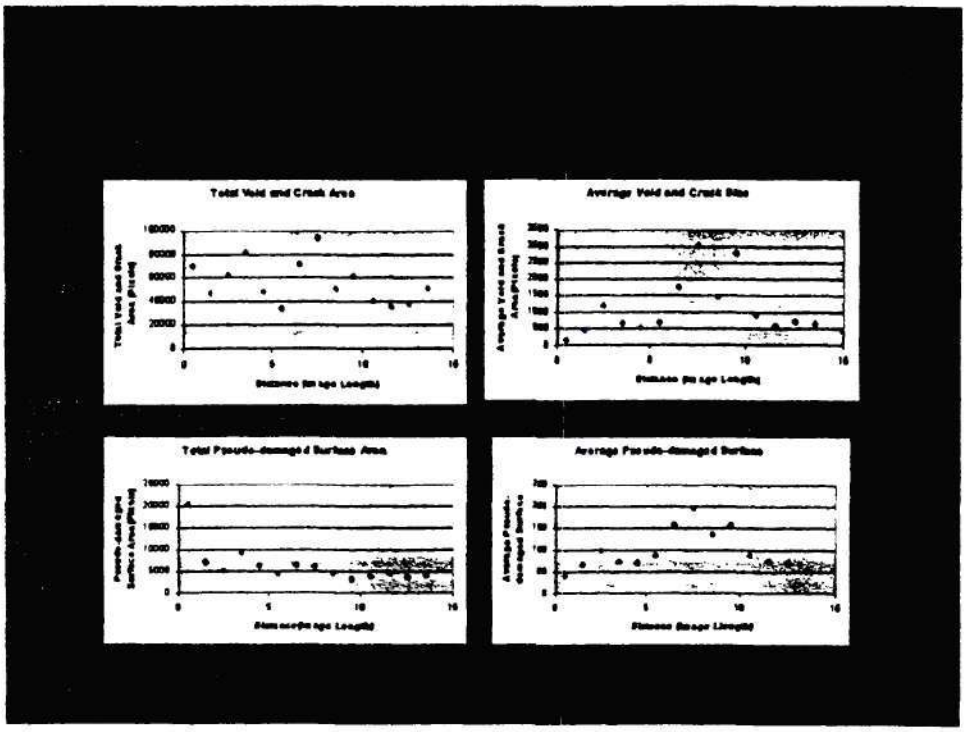

Figure 3.5.6 Cracked Area (Volume) and Pseudo-damaged Surface Area as a Function of Distance from the Tunnel

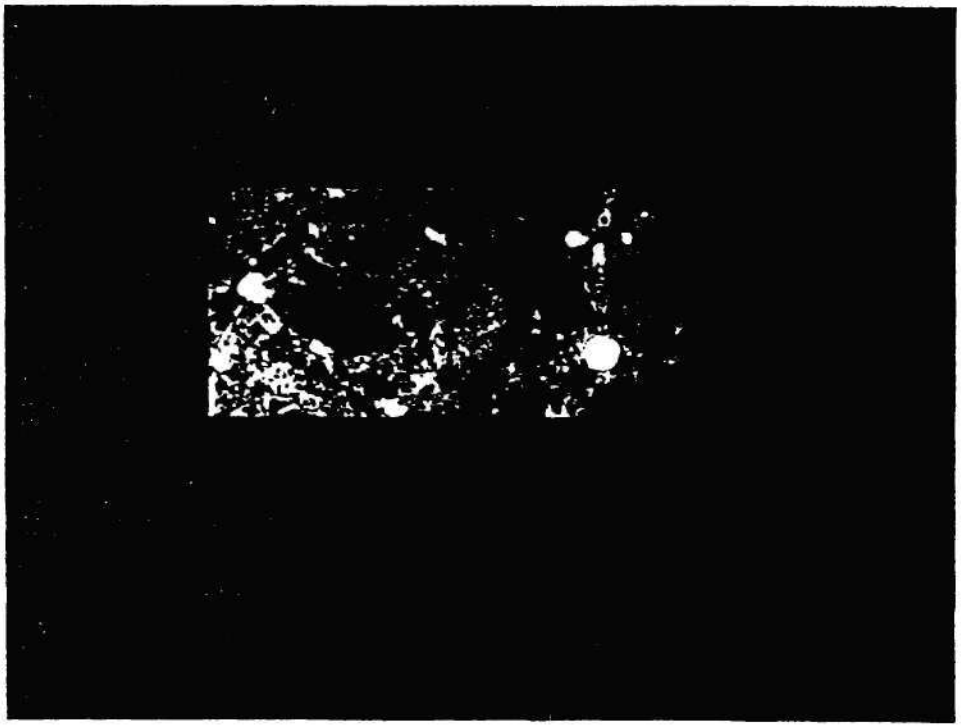

Figure 3.5.7 An Example for the Determination of the Mean Solid Path and Its Corresponding Tensor

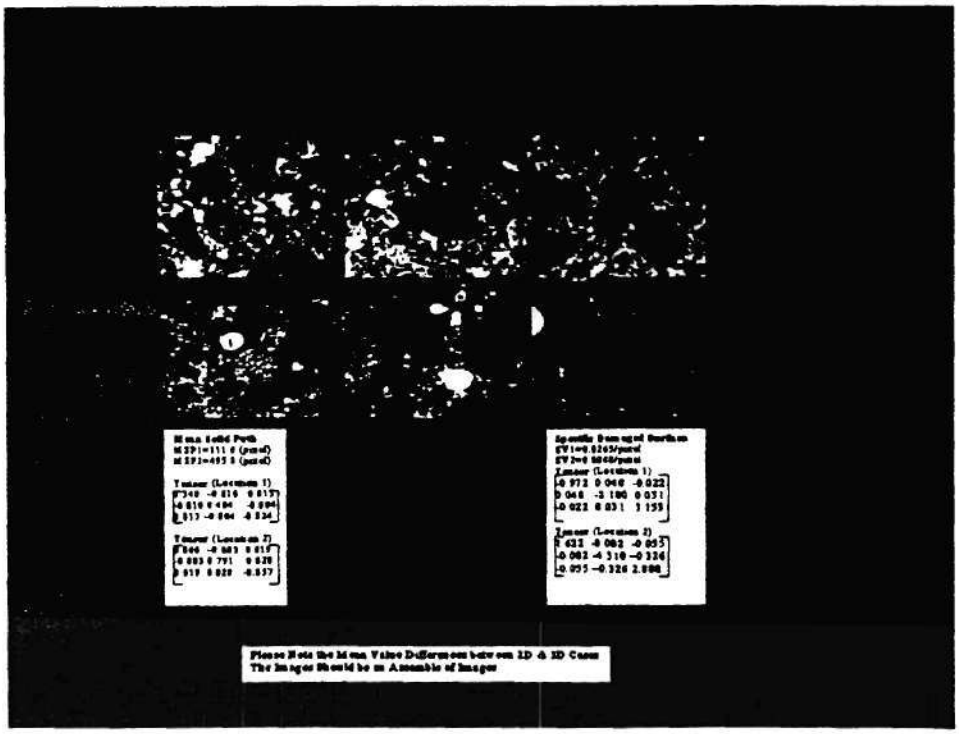

Figure 3.5.8 Example Determination of 3D Mean Solid Path Tensor and Specific Damaged Surface Area Tensor

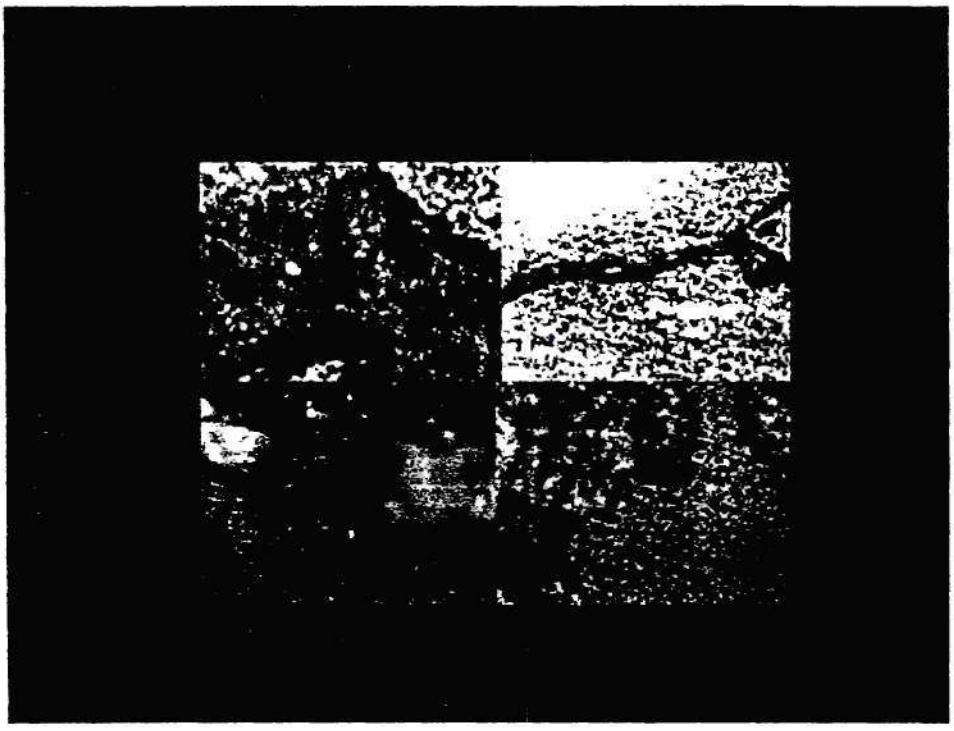

Figure 3.5.9 Illustration of Far Field Crack Characteristics

Metal Degradation and its Effects

Passage of a high-energy metallic projectile through concrete leads to development of significant microstructural damage in concrete at different length scales ranging from nanometers to centimeters. It also leads to deterioration in nose cone topography and associated local microstructure (see Figures 3.5.10a to 3.5.10d), and induces microstructural damage in the projectile. These microstructural and topographic changes may in turn affect the trajectory of the projectile through concrete. Therefore, it is of interest to quantify the microstructural and topographic changes in the metallic projectile resulting from its penetration in concrete. Based on this preliminary study, we noticed the necessity to apply advanced digital image processing techniques, digital profilometry, and stereology to quantify these aspects of damage evolution in the projectile material. It is proposed that the effects of the following variables on the damage development in the projectile be further studied:

1. Projectile alloy composition (steel versus tungsten heavy alloy)
2. Projectile geometry
3. Projectile energy
4. Concrete microstructure evolution adjacent to the projectile

The quantitative characterization will involve the estimation of the following parameters.

1. Changes in the surface roughness of projectile surface by using digital Profilometry and general stereological relationship developed by Gokhale and Underwood [Gokhale and Underwood, 1990].

2. Changes in the fractal dimension of the projectile nose-cone surface using the concepts of non-Euclidean geometry developed by Mandelbrot and coworkers [Mandelbrot and Passoja, 1984], and the experimental procedures developed by Gokhale and co-workers [Gokhale and Drury, 1990; Gokhale et al., 1993; Drury and Gokhale, 1993].

3. Estimation of metric properties of the three-dimensional microstructure using efficient stereological techniques [DeHoff and F.N. Rhines, 1968; Underwoood, 1970; Smith and Guttman, 1953; Baddeley et al., 1986; Gokhale and Drury, 1994].

4. Estimation of changes in the spatial arrangement of features in the projectile microstructure by using digital image processing and serial sectioning, and reconstruction of large-volume high-resolution three-dimensional microstructure from "montage" serial sections using the techniques recently developed by Gokhale and coworkers [Louis and Gokhale, 1995, 1996; Yang, et al., 1996, 1997].

a. Tungsten heavy alloy projectile in the concrete

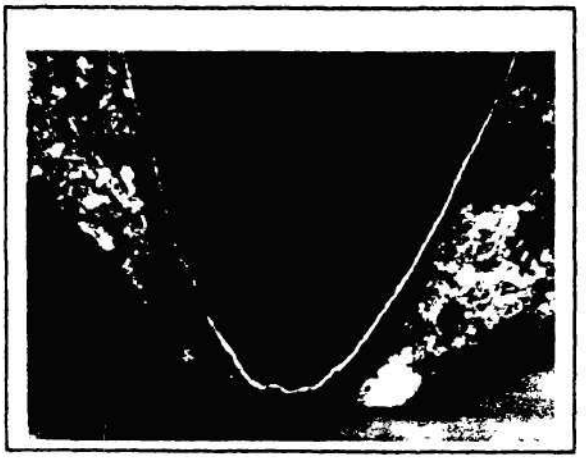

b. Deterioration in the topographic profile of the nose-cone of the projectile

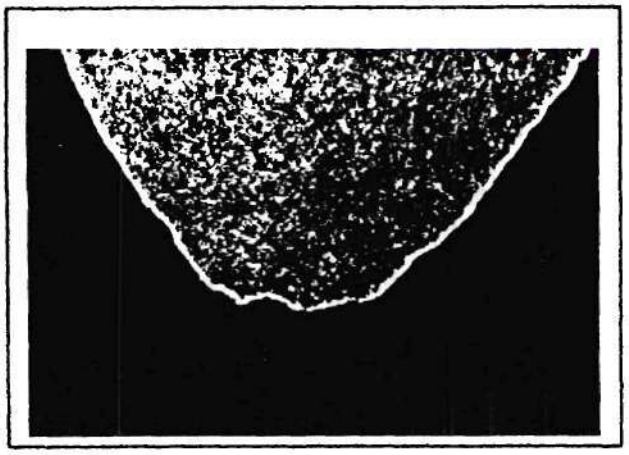

c. High magnification view of a

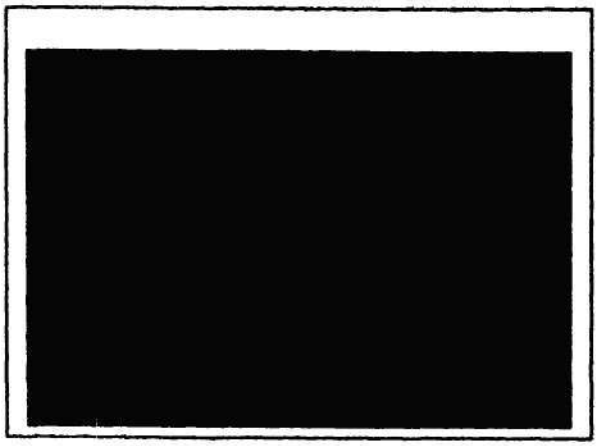

d. Localized deformation in metal at the projectile-concrete interface

Figure 3.5.10 Microstructure of Projectile Material

IV. PHASE II TECHNICAL OBJECTIVES, APPROACH AND WORK PLAN

As Phase II proposal has already been submitted, please refer to the Phase II proposal for details on objectives, approach and work plan. However, a brief description about these items is provided in this final report.

OBJECTIVES

The following Phase II technical objectives have been identified:

1. Develop methods to correlate the observed micro-structural damage parameters identified, developed and implemented in Phase I with macro-scale concrete material properties.

2. Integrate micro-structural damage analysis techniques developed and implemented during Phase I and utilized during Phase II into a user-friendly software package for automated data reduction.

3. Transition these micro-structural damage analysis techniques and software environment to AFRL for use in ongoing/future studies.

4. Submit a Phase III follow-on proposal for application of this technology for both the military and industry (i.e. construction, concrete material producers, civil engineering firms).

5. Prepare for third party commercialization of the software environment created during the Phase II effort.

WORK PLAN

To accomplish the technical objectives of the project, a series of tasks have been identified. It is noted that there are two parts to the proposed work plan: (a) Phase II; and (b) Phase II Option. The Phase II work plan focuses on the original SBIR topic, namely quantification of concrete microstructure evolution and correlation of microstructure with macro-scale properties. As a result of observations made during Phase I of this project, it is clear that an important parallel consideration is evolution of penetrator microstructure and the inter-relationship between this and the concrete microstructure damage. Accordingly, a Phase II Option focusing on the characteristics and damage of the penetrator is proposed herein. It is evident that a number of the tasks proposed in the Phase II plan can complement the Phase II Option plan. For example, concrete variables changed to study differences in concrete microstructure evolution and behavior could readily provide the necessary information to study differences in penetrator-concrete interactions also. For clarity, the Phase II and Phase II Option tasks are discussed separately herein but there is a strong technical justification to have them conducted in parallel.

Phase II Tasks:

Task 1: Complete Analysis of Existing Tested Target

One of the initial tasks of Phase II will be to conduct a complete analysis of an existing target using the imaging procedures outlined in Part 4 of this proposal. This would include a complete mapping of damage/microstructure at multiple scales. To accomplish this, the cutting scheme shown in Figure 4.1 is proposed. This scheme is based on observations made during Phase I of the project and indicates how analysis will be conducted on both discs (perpendicular to penetrator/tunnel direction) as well as well as on vertical faces of blocks cut from the cores. It is noted that similar cutting schemes will be used to study both the 7.5" tunnel cores as well as the 4" control cores. Further, it can be seen that montage generation is an integral part of the microstructure quantification procedure. It is also intended that analysis of select blocks would include montage generation on serial sections so that the true 3-D structure could be reconstructed digitally (Figure 4.2). Extensive details of the use of both the montage generation and serial sectioning procedures to study an alloy are provided in Part 6 of this proposal. The application of these methods to study concrete specimens would be very similar. The results of this Phase II task will allow for immediate verification of the procedures developed/implemented/identified in Phase I of the project as well as lead to a complete data set which can be used to identify enhancements to the proposed methods early in Phase II. The target to be studied in detail in this task would be selected by AWEF project personnel.

Task 2: Macro-Scale Property Testing of Concrete Specimen

In the same manner that Task 1 of Phase II will involve a complete quantitative microstructure analysis of an existing target, Task 2 will involve the performing of a complete macro-scale strength/modulus test program on an

existing core. This test program is based on a careful consideration of crack initiation and propagation mechanisms as summarized below.

The important macro-properties of concrete include compressive and tensile strengths, elastic modulus and bulk modulus, toughness and plastic deformation properties. Tensile strength and toughness are considered to be the most important properties under projectile penetration loading conditions. Both crack initiation and propagation are controlled by the toughness of aggregates, paste and ITZ. The compressive strength is actually controlled by the internal tensile stress of concrete. The important parameters of microstructure damage parameters for concrete include specific crack surface tensor, local volumetric fraction of voids, paste and aggregates, density of interfacial transition zone, mean free path, clustering, branching, fractal surface of voids and cracks, and bivariate void distribution. Among the microstructure damage parameters listed above, not every one of them has equal importance in its effect on different macro concrete properties. Quantification of various microstructure quantities may be conveniently implemented if high-quality images and automatic data reduction system can be developed. As many of the microstructure quantities can be quantified quite conveniently by the procedures we developed, we propose a multiple-factor correlation method for correlation analysis, which has not been achieved as a result of the lack of reliable quantification methods to date.

The following macro material properties will be determined from the core specimens taken from the target specimens.

- Dynamic elastic modulus (E_d) and dynamic shear modulus (G_d)
- Quasi-static elastic modulus (E_q) and Poisson's ratio (υ_q)
- Compressive Strength according to ASTM C 469
- Tensile strength from split tension test according to ASTM C 496

Figure 4.3 summarizes the scheme proposed for obtaining strength/modulus test cores from target specimens.

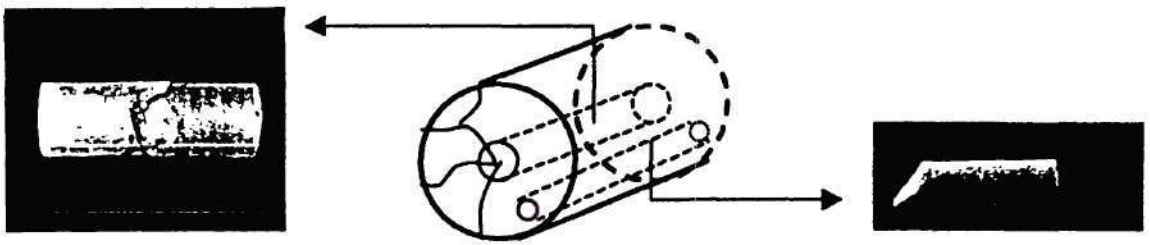

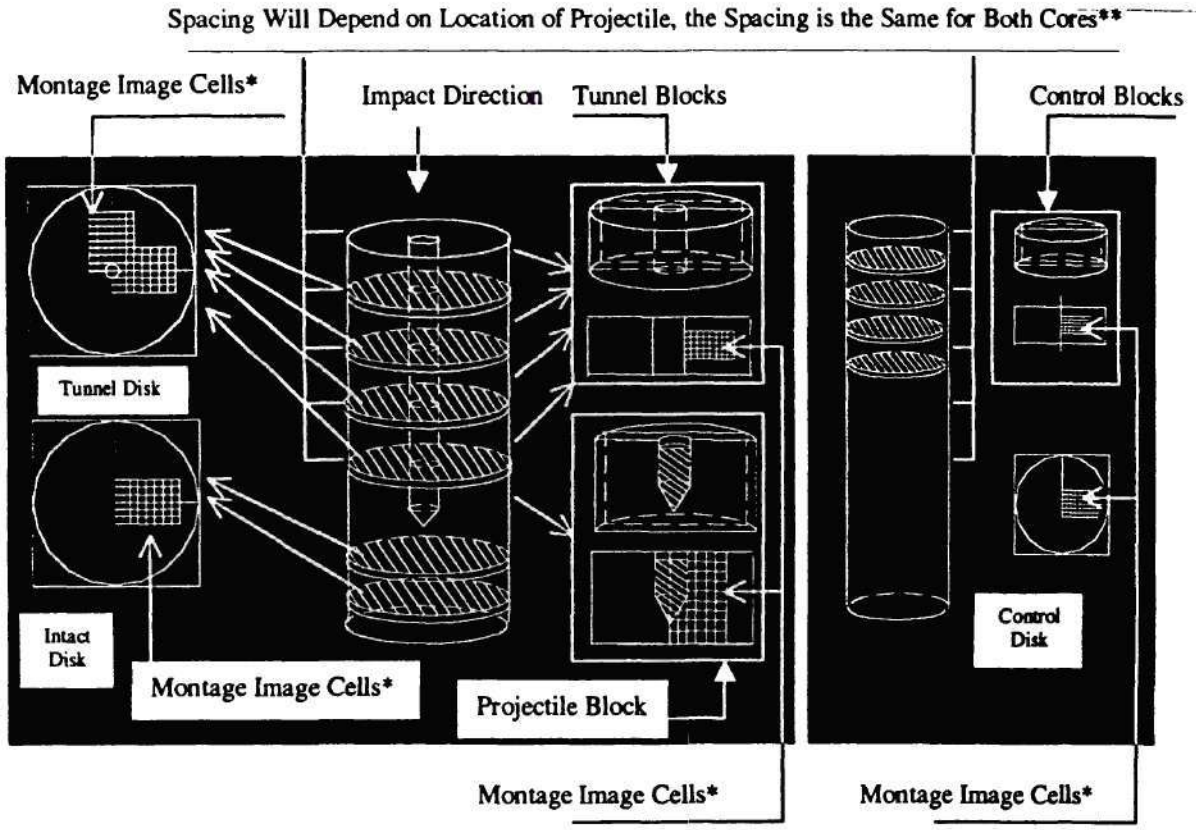

Note

* The sizes of image cells are dependent on the type of micro defects to quantify, the type of mixes, the typical magnitude of the micro defects and their density. Continuos image acquisition from the cells will be implemented. It is anticipated that at least 40-60 images shall be acquired, processed and analyzed for meaningful statistical evaluation of the micro defect distribution of any zone of interest.

** The spacing between the disks is dependent on the location of the projectile. However, it is anticipated that at least four disks for both tunnel disks and control disks shall be processed and analyzed. The number of the intact disks to analyze shall be dependent on the severity of damage ahead the tip of the projectile.

Figure 4.1 Sample Cutting and Observation Schemes for Both Tunnel and Control Cores

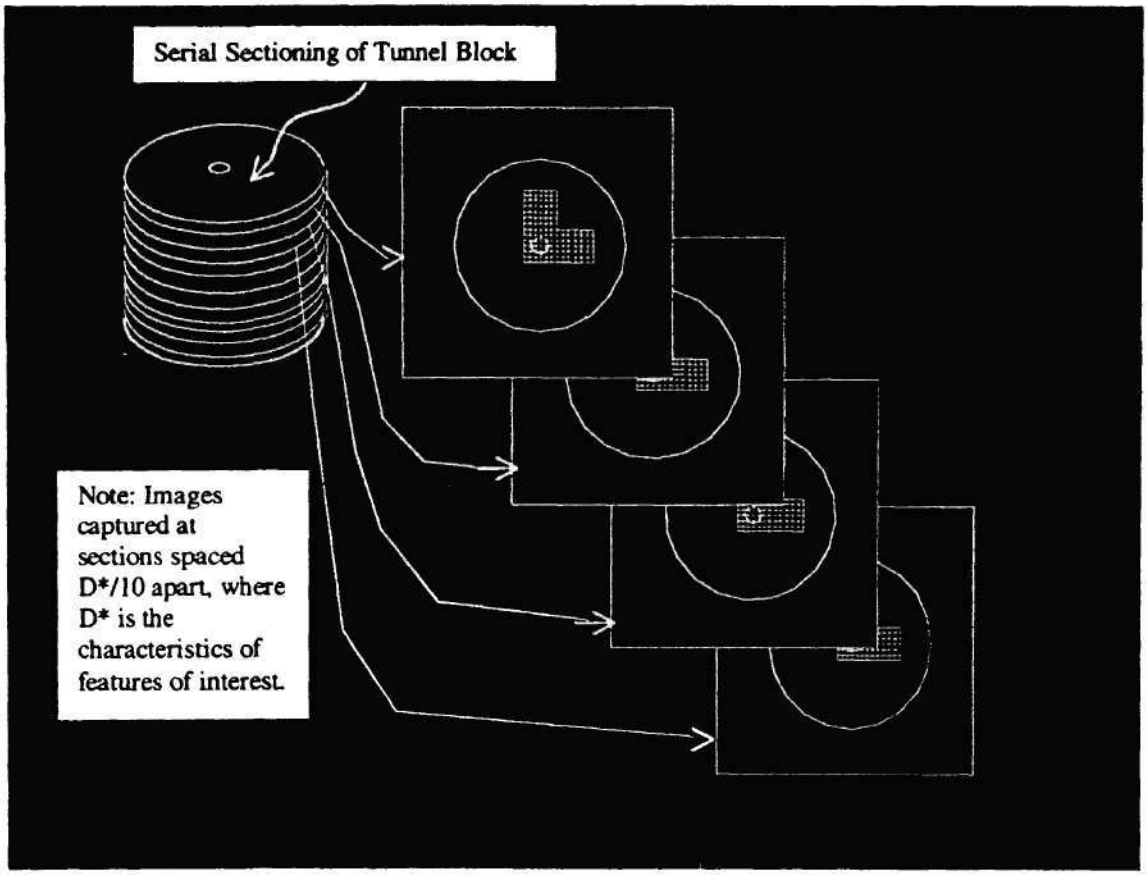

Figure 4.2 Illustration of Montage Generation Applied to Serial Sections of Tunnel Block

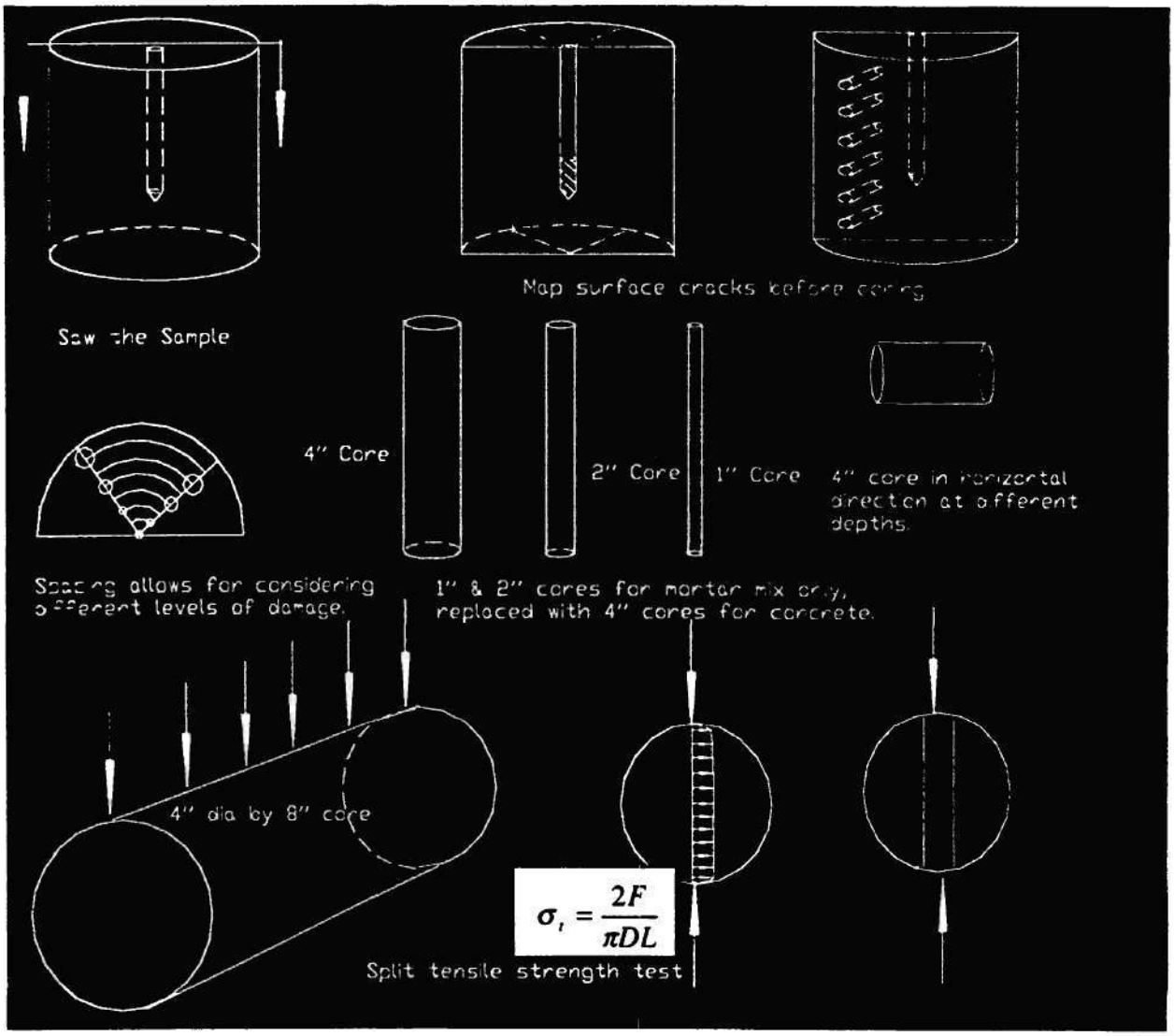

Notes

The following order should be followed:

1. Map macro surface cracks and reconstruct broken chunks.
2. Saw the cylinder into two pieces.
3. Map macro cracks on the revealed surfaces. Cut a thin section of the entire cross section for quantification of the micro crack distribution before coring.
4. The 1" and 2" cores are for the mortar mix sample only. Replace them with 4" dia. cores. Actual locations depend on the location of the macro cracks. The principle for choosing the core locations is to ensure the cores are representative of different damage levels in the sample.
5. Determine the effective properties and quantify the micro cracks.

Figure 4.3. Cutting and Coring Scheme

Task 3: Analysis of Target Boundary and Other Factors on Observed Damage

A critical component of any experimental procedure is the degree to which the measurements are free from apparatus effects. Based on both external evaluations of tested targets as well as observations of internal crack patterns from images at low and intermediate magnification made during Phase I of the project, there is strong potential that some of the damage features are the result of tensile stress waves which result when high impedance contrast boundaries are encountered. For example, a stress wave propagating in the concrete will encounter a large impedance contrast when it reaches the boundary and this can result in a tensile wave being reflected from the boundary (as opposed to a compressive wave) with the result that stresses within the concrete are doubled and this contributes to the amount of damage observed. Obviously the concern with this is that while the damage would be reflected in any quantitative micro-scale measurements, it would not be a factor in the macro-properties such as strength and modulus of virgin concrete that had not been subjected to penetrator induced loading. Accordingly, this task will use a combination of experimental, analytical and computational approaches to determine to what extent, the observed damage is influenced by the specimen boundary conditions and if so, whether the issue can be mitigated by some simple changes to the specimen boundary (e.g. inclusion of an stress wave absorption system at the boundary).

Task 4: Identification, Casting and Testing of Additional Targets

Having established the scope of damage-inducing conditions, Task 4 of the Phase II study will focus on identifying and performing additional tests necessary to allow for development of a broad relationship between concrete micro-structure and macro-scale properties. It is anticipated that both concrete and penetrator properties will be varied in these additional tests. As part of this task, the characteristics of available tested targets will be reviewed to minimize the number of targets to be tested.

This task will evaluate the macro-concrete material properties before and after the specimen is subjected to projectile penetration testing. The effects of different types of concrete (normal strength concrete, high performance concrete, and normal strength mortar), projectile type and impact velocity will be evaluated. The factors to be evaluated in this proposed program include the following:

Concrete Mixes (3 different):

- Normal strength concrete, 5000 psi compressive strength, #57 crushed granite aggregate
- High performance concrete, 10000 psi compressive strength, #57 crushed granite aggregate, silica fume and superplasticizer
- Normal strength mortar, 5000 psi compressive strength, #8 max. aggregate size.

Projectile size / Striking velocity (various factors to be decided by AWEF project personnel):

The objectives of using three different concrete mixes are twofold. Different maximum aggregate size (No 57 versus #8) will develop different characteristics in the drying shrinkage crack and the interface transition zone properties and would respond differently under the projectile penetration loading. The use of high performance concrete will achieve two objectives. One of the project team members has developed several high performance concretes with strengths ranging from 8000 psi to 18,000 psi [Lai et. al. 1999]. Silica fume and superplasticizer were used in all the high performance concrete. In addition to the high strength, the fresh concrete properties of all the high performance concretes are significantly different from the normal strength concrete. For normal strength concrete bleeding normally occurs and as a result, the interface between the aggregate and the paste is weak and is susceptible to shrinkage cracking. For high performance concrete, due to the use of silica fume and low water-to-cement ratio, the available mixing water is absorbed by the silica fume and as a result no bleeding occurs in the concrete mix. This could significantly change the propensity of shrinkage cracking and the interface characteristics between the aggregate and the paste. In addition, the strength of the high performance concrete paste phase is as strong or stronger than that of the aggregate. All of these could significantly change the microstructure of the concrete and could significantly improve the performance of the concrete under the projectile penetration loading. The crack arresting effects of coarse aggregates, the paste, and the effects on ITZ property improvement by silica fume and low water-to-cement ratio will be evaluated.

The objective of using projectiles with different sizes and different striking velocities is to investigate the microstructure damage effects caused by these different projectiles. (Note this is also complimentary to the objectives of the Phase II Option work plan. If the projectile sizes and the striking velocities can be independently selected, then two different projectile types and two different velocities will be selected. As different striking velocities will represent different strain rates, strain rate effects on damage can be investigated as well. The purpose of using different sizes of projectile is to investigate scaling effect of projectile penetration tests. As was illustrated by Bar [1997], geometric proportionality does not result in proportionality between energy consumption on surface phenomena and that on volume phenomena required for scaled experiment. This test could provide useful information on how to evaluate the damage effects of full-scale penetration test (a missile penetrating into a concrete target) from those observed in scaled tests. Combining the information obtain from this experiment with numerical simulation techniques may present a solution to the scaling effect problem.

Concrete Specimen Preparation

The proportions for the three concrete mixes will be developed by the project team to ensure the mixes will have adequate workability for the concrete to be produced by a ready mix concrete plant and the mixes achieve the specified strength. For the high performance concrete to be used for this project, one of the mixes developed in a previous research project [Lai and Kahn, 1999] can be used directly.

After the mixes have been successfully produced in the laboratory theses mixes will be produced by a local ready mix concrete producer who has experience with preparing high performance concrete. The following specimens will be cast for each concrete mix.

- Three target specimens: 30" diameter by 36" long
- 12 standard cylinder specimens: 4" diameter by 8" height.

During the first 72 hours after casting the target specimen and 3 of the 4" by 8" cylinder specimens will be covered to prevent loss of moisture, and cured in the concrete form. After 72 hours the forms will be removed, and the target specimens will be placed in the outdoor open air environment for at least 1 month. For the remaining 4" by 8" cylinders, the specimens will be subjected to standard ASTM curing conditions according to the procedures specified in ASTM C 192. Additional details of studies to be performed on these cylinders are discussed in Task 6 also.

Penetration Tests

After the target specimens have been cured for at least one month, two target specimens for each mix will be shipped to Eglin Air Force Base for projectile penetration testing. The remaining target specimen for each mix will stay at Georgia Tech and will be used as a control specimen. The projectile penetration testing will be performed at the Advance Warhead Experimentation Facility. The projectile types and the testing parameters, such as the striking velocity, will be determined by the program manager.

Post Penetration Evaluation

After target specimens have been tested at the Advanced Warfare Experimentation Facility, they will be carefully examined by Global Technology/Georgia Tech personnel before being shipped back to Atlanta for more detailed testing and analysis. Measurements of bulk target damage will be made and procedures implemented to stabilize the specimens before the desired cores are obtained. For all the target specimens subjected to projectile penetration testing the surface cracks, broken chunks, fractured surfaces will be mapped, reconstructed, and quantified using the techniques identified during Phase I study. The information obtained for the entire specimen will permit comparison with numerical simulations.

Samples from different locations and at different orientations with respective to the direction of projectile penetration will be taken from the damage target specimens as previously shown in Figure 4.3. The same coring will be made on the control target specimens so that the effects due to shrinkage and other factors not associated with projectile penetration damage can be separated from that due to the projectile penetration. As previously

noted, existing targets will also be evaluated to ensure that a sufficiently large database of microstructure and macro-scale properties is available.

Task 5: Analysis and Correlation of Microstructure Damage with Macro Material Properties

The various Phase II tasks are expected to provide a large data set which can be used to correlate microstructure properties with macro-scale material properties of a range of different concrete mixes (new mixes as well as those previously tested by AWEF). The microstructure and macro-scale measurements will reflect both inherent as well as induced properties.

Two of the four linear elastic material parameters, elastic modulus, bulk modulus, shear modulus and Poisson's ratio will be determined directly. Once two of them are know, the remaining two other parameters can be determined from the linear elastic theory. Therefore all four elastic material properties for the various concretes before and after the projectile penetration testing are available at different locations in the target specimens. The microcrack characteristics and distributions at the same locations have also been quantified. Correlation between the microcrack-induced damage on the macro elastic properties can be developed. For example, the relations in equation (1) and (2) developed by Bundiansky and O'Connell (1976) can be justified as the size and orientation distribution can be validated.

$$\frac{\bar{K}}{K} = 1 - [2N < a^3 f(\bar{\nu}) > /[3(1-2\bar{\nu}] \qquad (1)$$

$$f(\bar{\nu}) = \frac{4\pi}{3}(b/a)^2 (\frac{1-\bar{\nu}^2}{E(k)}) \qquad (2)$$

where $K, \bar{K}$ are the bulk modulus of undamaged materials and effective bulk modulus with damages. $N < a^3 f(\bar{\nu}) >$ represents the size distribution of cracks, $\bar{\nu}$ is the effective Poisson's ratio, $f(\bar{\nu})$ is a function of $\bar{\nu}$ and $E(k)$ is an elliptical integral. See Bundiansky and O'Connell (1976) for details. These parameters can be also related to the damage parameter C_d, see Taylor (1986).

Task 6: Comparison of Indirect and Direct Tensile Strength Test Results

As part of the concrete macro-scale test program, it is proposed to use both indirect tensile tests (Brazilian Tests) as well as unconfined extension and compression tests on cylindrical specimens. One task of the project will be to specifically compare strength and modulus results from these different types of tests with the quantitative micro-structure measurements. Use of the split tension test for determining the tensile strength of brittle materials offers many advantages over the direct tension test, particularly in terms of ease of the testing. As a result, the split tension test has been used widely for determining the tensile strength of concrete. However, due to the stresses induced in the specimen under the direct tension and the split tension are significantly different resulting in significant different in the scaling effect and the influence of the microcracks in the concrete on the results of the tensile strength determined from the direct tension and the split tension. Use of the imaging analysis in conjunction with the testing of the macro material properties offer a unique opportunity to quantify the effects of these two different tests for determining the tensile strength of concrete and other brittle materials. The tensile strength will be determined for the concrete materials from the cores taken at different location in the target specimens before and after the projectile penetration testing. The reason for determining the tensile strength from both the direct tensile test and the split tension test is that the influence of microcracks in the specimen is significantly different on the direct tension test and the split tension test. For instance those microcracks outside the diametral region of the specimen, (see Figure 4.3), has minimum effect on the tensile failure of the specimen, while for the direct tension test, the microcracks in the entire specimen would affect the tensile failure of the specimen. Therefore, correlation of the microcracking properties with the tensile strength from the direct tension test and split tension test can be very important. This task will thus help establish the significance of this factor given that standard test procedures are based on extension and compression tests on cylindrical specimens yet indirect tests are commonly used in practice.

Task 7: Influence of Curing Conditions on Micrsotructure

At the time of casting additional target specimens for testing, concrete cylinders (4" diameter) will be cast and cured as previously noted. This task will compare micro-structure and macro-scale properties for these cast cylinders with the microstructure and macro-scale properties of cylindrical specimens of the same diameter cored from the larger target specimens. This task will allow the influence of curing conditions on the micro-structure to be evaluated. Standard procedures for determining macro-scale properties such as strength and modulus specify the casting of cylinders. Without this task, the validity of measurements and hence macro-scale to micro-structure relationships based on specimens cored from targets can not be assessed. The overall experimental approach for evaluating both existing and new targets is summarized in the flow-chart shown in Figure 4.4

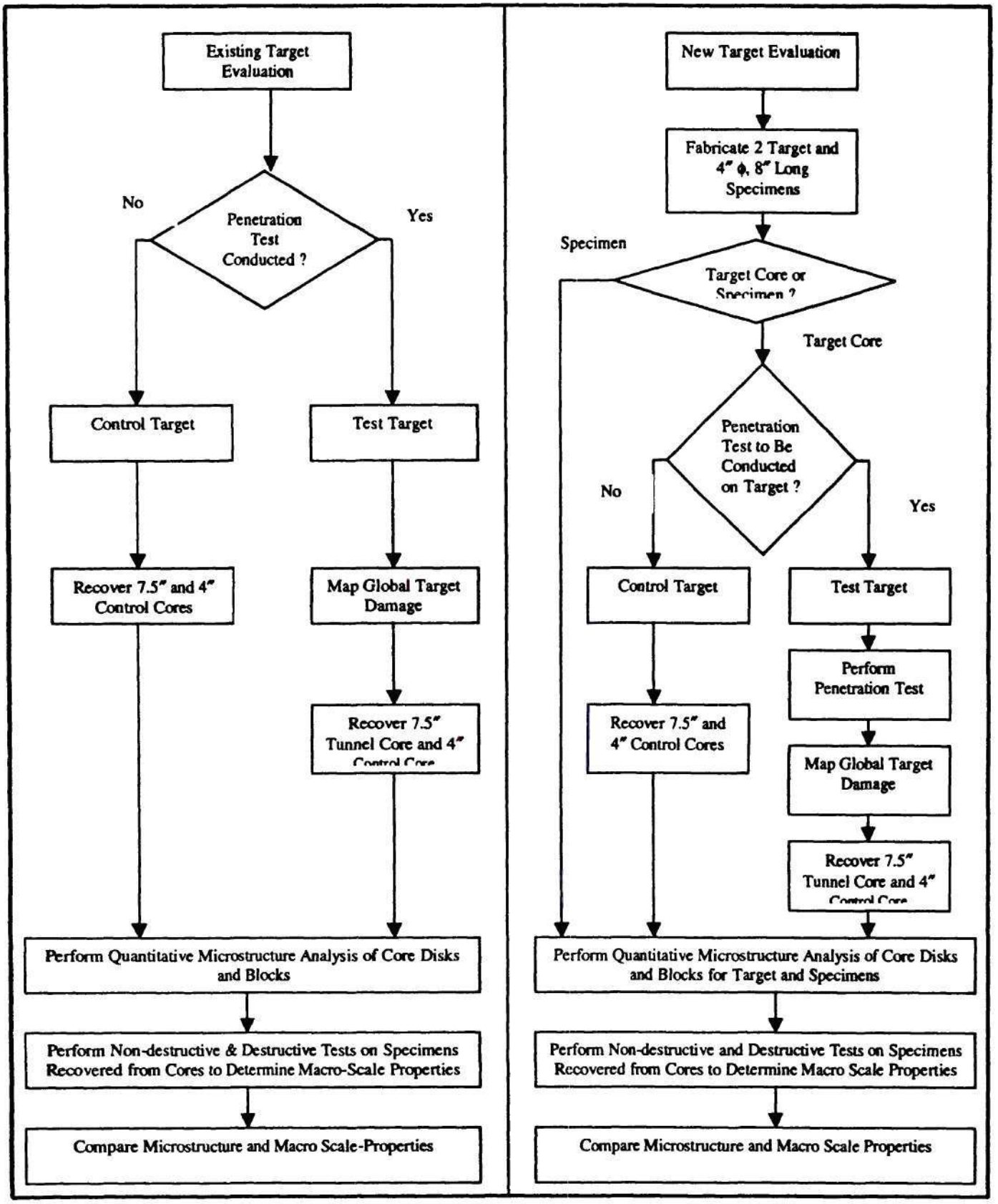
Existing Target Evaluation
Penetration Test Conducted ?
No
Yes
Control Target
Test Target
Recover 7.5" and 4" Control Cores
Map Global Target Damage
Recover 7.5" Tunnel Core and 4" Control Core
Perform Quantitative Microstructure Analysis of Core Disks and Blocks
Perform Non-destructive & Destructive Tests on Specimens Recovered from Cores to Determine Macro-Scale Properties
Compare Microstructure and Macro Scale-Properties
New Target Evaluation
Fabricate 2 Target and 4" ϕ, 8" Long Specimens
Specimen
Target Core or Specimen ?
Target Core
Penetration Test to Be Conducted on Target ?
No
Yes
Control Target
Test Target
Perform Penetration Test
Recover 7.5" and 4" Control Cores
Map Global Target Damage
Recover 7.5" Tunnel Core and 4" Control Core
Perform Quantitative Microstructure Analysis of Core Disks and Blocks for Target and Specimens
Perform Non-destructive and Destructive Tests on Specimens Recovered from Cores to Determine Macro Scale Properties
Compare Microstructure and Macro Scale Properties

Task 8: Integration of Quantification Algorithms into Software Environment

When the relevant micro-structure quantifiers have been fully identified through the various preceding tasks, an integrated software package which will allow for user-specified analysis of images at various scales will be developed. This software environment will reflect consideration of the needs of the project sponsor as well as a broader community that would use a commercialized version of this product. A modular framework is being proposed for this software. This is to allow development of code to be initiated early in the project. In addition, this has the benefit of significantly extending the commercial attractiveness of the software since it can be readily enhanced as new quantification algorithms are developed or as existing algorithms are enhanced.

Task 9: Synthesis of Phase II Developments

The final task of this Phase II study will be the preparation of a synthesis report which will summarize the developments and findings of Phase II. This report will be a key component for identifying critical issues likely to enhance the potential for commercialization of the product.

PHASE II OPTION WORK PLAN

The objectives of the Phase II Option are to quantify the microstructural and topographic changes in the metallic projectile resulting from its penetration in concrete. Advanced digital image processing techniques, digital profilometry, and stereology to quantify these aspects of damage evolution in the projectile material. It is also proposed to study the effect of the following variables on the damage development in the projectile.

1. Projectile alloy composition (steel versus tungsten heavy alloy)
2. Projectile geometry
3. Projectile energy
4. Concrete microstructure

The quantitative characterization will involve the estimation of the following parameters.

1. Changes in the surface roughness of projectile surface by using digital Profilometry and general stereological relationship
2. Changes in the fractal dimension of the projectile nose-cone surface using the concepts of non-Euclidean geometry
3. Estimation of metric properties of the three-dimensional microstructure using efficient stereological techniques
4. Estimation of changes in the spatial arrangement of features in the projectile microstructure by using digital image processing and serial sectioning, and reconstruction of large-volume high-resolution three-dimensional microstructure from "montage" serial sections

See our Phase II proposal for more details.

V. Phase III - Contemplated Potential Commercial Products

A. Capability of the Offerer to Commercialize Technology:

Dr. A.B. Thakker has a track record of bringing technology to marketplace and exploiting its commercial potential. Prior to his association with GTC, he headed Commercial Technology group for Rolls Royce, Inc. in Atlanta for three years. He marketed and commercialized Rolls Royce developed technology such as: thermal indicator points, smoke meter, single crystal orientation measuring device, etc. He is a registered civil engineer in the states of Florida and Virginia, and understands the technical and business issues related to commercialization. GTC has can bring its sales and marketing experience to bear on the commercialization of this product.

B. Commercial Intent

Global Technology Connection, Inc. is a for-profit corporation and is committed to technology transfer/commercialization of technology developed under this contract. The targeted commercial venture does not rely on continued SBIR funds. In addition to its own resources, GTC will solicit funds from third party angel investors or venture capital funds to partially fund Phase III. Also, targeted would be funds from Georgia Research Alliance, a state level program to assist small companies participating in SBIR programs. GTC being a potential Advanced Technology Development Center (incubator established by the State of Georgia) company would have at its disposal financing assistance networks established by ATDC to help high technology companies.

The Advanced Technology Development Center (ATDC) has objective to speed up the rate of successful commercialization of R&D. This is accomplished via a process which contains the following components:

- comprehensive business research and strategic planning,
- developing a business plan, a stand-alone Executive Summary, and presentation materials,
- targeted outreach to potential strategic allies and investors, and
- commercialization Opportunity Forum which brings together well-prepared technology entrepreneurs with prequalified investors and teaming partners.

The success of this program is measured by the success of our clients. Specifically, we look at:

- how many finalists receive private sector financing within 18 months of the Forum,
- the dollar value of those signed agreements

- the dollar value of increased sales, and
- the increase in the number of jobs.

Several other Phase II partners like Law Engineering, concrete companies will be approached for Phase III funding. Law Engineering Group has already shown their commitment for the Phase II effort.

GTC also participates with Georgia Technology Alliance (Group made up of active angel investors, VCs , State agencies, high technology startup companies). Maximum exposure to this group will be available for Phase III funding and partnership. This will assure connection to private sector sources of early-stage technology financing and assistance in technology commercialization. .

Also, other procurement/R&D/phase III(non SBIR) opportunities in DoD and the rest of government will be solicited. Some DoD components have started Phase II plus type of funding. The general concept is to provide qualified Phase II businesses with additional Phase II SBIR funding if they can obtain matching non-SBIR funds from acquisition programs, the private sector, or both. This mechanism, if available for this program will be explored.

Market Assessment

It is envisioned that just 100 customers can provide $1M revenue a year in annual licensing and support service contracts. This projection was arrived modest sales and support projection. The ultimate market size is anticipated to be far greater than 1500-2000 ongoing customers worldwide. This target market to be realized in five years after completion of Phase III

This target market will consist of:

- USAF (Munitions) and other DoD Components
- Other Government agencies (Corps of Engineers, Federal Highway Administration)
- Ammunition manufacturers
- Concrete material users producers
- Geo-material users and producers
- Construction Industry
- Earthquake / Hurricane Damage Assessment (Insurance Companies/Attornies)

- Life Prediction and Durability Assessment of Concrete and Geo-Materials
- Aggregate Particle Sizing and Shape Measurement
- Pavement Mix Durability Enhancement

There are no current or potential known competitors that have targeted this market. It is envisioned that initial capital of $250K would be required to market this technology to some targeted customers. PTI (subsidiary of ASTEC company) has already given commitment of 100K to market and commercialize this technology as a Phase III partner. Additional funds will be sought from potential investor/ non SBIR government funds or internal company funds.

PTI has successfully designed and commercialized a number of products related to materials sampling, testing and quality control equipment. PTI's previous success in the commercialization of products and their reputation in the industry will further enhance the commercialization of this SBIR effort.

VI CONCLUDING REMARKS

As a result of Phase I work, the feasibility of adapting and implementing a range of specimen preparation and image analysis techniques developed by members of the project team has been demonstrated. These range from epoxy impregnation, differential pressure polishing and bright-field microscopy techniques used for preparing and capturing images to development/adaptation of morphological processing algorithms which enable properties such as the local volume fraction, surface area density, connectivity and mean free-path to be automatically quantified from high-quality images. Use of these techniques in conjunction with other proven procedures such as serial sectioning and montage creation developed by members of this project team will enable multi-scale high resolution quantification of micro-structure damage for large areas and volumes of concrete to be successfully conducted. More importantly, the application, during Phase I, of many of these techniques to coupons cut from an actual tested target have demonstrated the need for careful consideration of factors such as target boundary effects, concrete mix design, penetrator-concrete interactions and concrete strength/modulus test procedures during the early stages of Phase II. It is evident that without such related considerations, correlation's between conventional macro-scale properties such as strength and modulus and measured micro-structure quantities for targets after penetration may be sufficiently masked by boundary effects and other test conditions that implementation of the technology developed will be flawed. On summary, the achieved objectives were detailed as follows:

1. Development of sample preparation techniques that include cutting, grinding, polishing, grinding with coated epoxy, image filtering and bright field imaging. The effects of these techniques on image quality have been visually illustrated in this report. The techniques developed are economic and efficient.

2. State-of-art techniques for sampling large area and volume at high resolution including image montage generation and serial sectioning developed by the team members have been successfully adapted to the application in this concrete project.

3. A thorough literature review has been performed to identify the microstructural features and parameters that most significantly affect the macro properties such as strength, modulus and fracture toughness. These features and parameters include the density and orientation distribution of cracked surface area, voids, local volume fractions, bivariate size and orientation distribution of cracks, the mean solid (free) path, fractal dimension and branching of cracks etc. The format of these quantities have been so chosen that they can be directly applied in continuum damage mechanics, micromechanics and fracture mechanics to predict the macro properties and develop constitutive models that include these parameters as internal variables.

4. Various computer programs have been adapted or newly developed to automatically reduce data from images to obtain the microstructural quantities. These programs can be conveniently assembled into an integral

computer software for Phase II studies. Examples have been given in this report to demonstrate the application of these programs.

5. A special effort has been directed to the study of the degradation of the projectile material during penetration process.

Several findings that are considered relevant for the Phase II study are emphasized here:

1. The Phase I experimental work and evaluations have added to the opinion that the amount and characteristics of damage present in the target specimens is influenced by boundary conditions. As stress waves induced by the penetrator impact propagate through the target, they are affected by changes in impedance they encounter. Clearly, one of the larger changes they encounter is when they reach the edge of the specimen. Reflected tensile stress waves resulting from this change in impedance are believed to be a significant contributor to the overall damage observed. Accordingly, quantitative measures of microstructure will reflect damage due to this tensile wave however macro-scale strength and modulus properties measured on intact specimens will not reflect this behavior. As a result, any correlations developed will have questionable validity. Accordingly, it is suggested that one of the tasks for Phase II should be to conduct specific analyses to assess the significance of boundary effects and depending on the outcome of these studies, to identify procedures which could be used to mitigate/reduce this effect.

2. Obviously, a major portion of the proposed Phase II work is the actual evaluation of micro-scale damage in target specimens. However, to prevent misleading information from being included in the correlation, unique procedures developed by members of the project team that allow high-resolution images of large areas to be created for subsequent quantitative analysis are important. This technique, which is called montage generation, enables features which extend across several adjacent images to be quantified in their entirety and is critical in the present studies since the magnification required to observe smaller linear features such as micro-cracks results in them crossing multiple image boundaries. Similarly, using the montage procedure in connection with three-dimensional serial sectioning procedures will allow the true characteristics of many critical features to be accounted for in comparing microstructure and macro-scale properties. Studies conducted during Phase I have indicated that without the use of such procedures, quantitative measures of microstructure will not be correct and consequently, any correlations with macro-scale properties will be ill-conditioned.

3. Since a key component of Phase II will be correlating macro-scale properties such as modulus and strength with quantitative measures of microstructure, it is also proposed to assess aspects of the procedures used to determine the macro-scale properties. Evaluations conducted as part of Phase I have shown that the volumes of material involved in determining the strength of a concrete specimen are a function of the test method. For example, while the entire specimen is loaded in a conventional cylindrical extension test, only a portion of the

specimen is stressed in the indirect strength test. Although these procedures generally give comparable macro-scale measures, clearly the assumption that the microstructure is consistent throughout the specimen is uniform needs to be evaluated. For example, it is expected that the microstructure of a cast 4" diameter cylinder will be different than the microstructure of a 4" cylinder cored from the center of the target which is in reality a 30" diameter cast cylinder. Variations in the curing conditions as a result of the relative sizes of these cast cylinders can undoubtedly influence the validity of correlations between quantitative microstructure measurements and macro-scale properties.

4. In the course of conducting Phase I of the project and discussions with project personnel from the Advanced Warhead Experimentation Facility, it is clear that additional study of the role of the characteristics of the penetrator (e.g. material, shape) were considered to be of significant interest also. Accordingly, it is proposed that Phase II program should include this aspect of the problem. It is considered that the induced microstructure is a complex penetrator-concrete interaction problem where the results of specific studies on the concrete can only be enhanced by parallel consideration of penetrator performance issues. Taking this approach would allow for both issues to be studied using the same tests and techniques.

VII REFERENCES

Abell, A.B. and Lange, D.A. (1998). Fracture Mechanics Modeling Using Images of Fracture Surfaces. **Int. J. Solids Structures**, Vol.35, Nos. 31-32, pp4025-4033.

Baddeley, A, Gundersen, H.J.G. and Cruz Orive, L.M.(1986). "Estimation of Surface Area From Vertical Sections",**Journal of Microscopy**, Vol.142, PP.259-276.

Benes, V., Jiruse, M. and Slamova M.(1997)."Stereological Unfolding of the trivariate Size-Shape-Orientation Distribution of Spheroidal Particles" **Acta Materialia**, Vol. 45, PP. 1105-1113.

Cahn, J.W.(1967). **Trans. Met. Soc. AIME**, Vol.239, PP. 610-616.

Chudnovsky, A. and Wu, S.F. (1990). Effect of Crack-Microcrack Interaction on Energy Release Rates. **Int. J. Fracture**, Vol. 44, pp43-56..

Cruz Orive, L.M.(1976)."Estimation of Size-Shape Distribution", **Journal of Microscopy**, Vol.107, PP.235-240..

DeHoff, R.T. (1962) "Estimation of Size Distribution of Ellipsoidal Particles From Metallographic Sections", **Trans. Metal. Soc. AIME**, Vol.224, PP.474-478.

DeHoff, R.T.(1967). **Trans. Met. Soc. AIME**, Vol.239, PP. 617-623.

DeHoff, R.T. and Rhines, F.N.(1968). Quantitative Microscopy, McGraw-Hill, New York, NY.

Dighe, M. D., Jiang, X.G., Rahardjo, A.S.B., Tewari, A. and Gokhale, A.M. "Quantitative

Microstructural Analysis of Porosity in A356 Alloy", **Trans. American Foundrymen's Society**, in press.

Drury, W.J. and Gokhale, A.M.(1993) "Measurement and Interpretation of fracture Surface Fractal Dimension", **ASTM STP no. 1165**, PP. 295-310.

Gokhale, A.M.(1990)."Unbiased Estimation of Curve Length From Vertical Slices", **Journal of Microscopy**, Vol.159, PP.133-141.

Gokhale, A.M. and Underwood, E.E. (1990). "A General Method for Measurement of Fracture Surface Roughness", **Metall. Trans.-A**, Vol.21A, PP. 1191-1199.

Gokhale, A.M. and Drury, W.J.(1990). "A General Method for Measurement of Fracture Surface Roughness-II: Practical Aspects", **Metall. Trans.-A**, Vol.21A, PP. 1201-1207, 1990.

Gokhale, A.M.(1992). "Estimation of Length Density From vertical Slices of Unknown Thickness", **Journal of Microscopy**, Vol.167, PP.1-8.

Gokhale, A.M., Drury, W.J. and Mishra, S. (1993). "Recent Developments in Quantitative Fractography", **ASTM STO no.1203**, PP. 3-22.

Gokhale, A.M. and Drury, W.J.(1994). "Efficient Estimation of Microstructural Surface Area using Trisector", **Metall. Trans.**, Vol.25A, PP.919-929.

Gokhale, A.M.(1996)."Estimation of Bivariate Size and Orientation Distribution of Microcracks", **Acta Materialia**, Vol. 44, PP. 475-485.

Gokhale, A.M.(1998). "Estimation of Integral Mixed Surface Curvature From Vertical Sections", **Acta Materialia**, Vol.46, PP. 1741-1748.

Gokhale, A.M., Tewari, A. and Miracle, T.H.(1998)."Effect of Gravity on Evolution of Spatial Arrangement of Features in Microstructure: A Quantitative Approach", **Proceedings of NASA Microgravity Materials Science Conference**, Huntsville, Alabama, NASA Conference.

Holmquist, T.J., Johnson, G.R. and Cook, W.H.. (1995) A computational constitutive model for concrete subjected to large strains, high strain rate, and high pressures. **Proceedings of 14th International Symposium on Ballistics**, Quebec City, Canada.

Jang, D.J., Frost, J.D., and Park, J.Y., (1999), "Preparation of Epoxy Impregnated Sand Coupons for Image Analysis", ASTM Geotechnical Testing Journal, Vol. 22, No. 2, pp. 153-164.

Kanatani, K.I. (1984a). Stereological determination of structureal anisotropy. **Int. Engng. Sci.** Vol.22,No.5,pp531-546.

Kanatani, K.I. (1984b). Stereological determination of structureal anisotropy. **Int. J. Engng. Sci.** Vol.22, No.5,pp531-546.

Kanatani, K.I.(1985). Distribution of Directional Data and Fabric Tensors. **Int. J. Engng. Sci.** Vol.22,No.2,pp149-164.

Keppel, E.(1975) "Approximating Complex Surfaces by Triangulation of Contour lines", **IBM Journal of Research & Development**, Vol 19, No. 1, PP2-11.

Krajcinovic, D. (1984). Continuum Damage Mechanics. **Applied Mechanics Review**, Vol.37, No.1, pp.1-6.

Krajcinovic, D. and Fanella, D. (1986). A Micromechanical Damage Model for Concrete. **Engineering Fracture Mechanics**, Vol. 25, Nos.5/6, pp.585-596.

Lai, J.S., Kahn, F.K., "Mix Design and Properties of High Performance Concrete" **Technical Report**, School of Civil and Environmental Engineering, Georgia Tech, June 1999.

Liu, G., Yu, H. and Li ,W.(1994).Efficient and Unbiased Evaluation of Size and Topology of Space Filling Grains", **Acta Stereologica**, Vol. 13, PP. 281-286.

Lorensen, E.W. and Cline, H.E. (1987) "Marching Cubes: A highresolution 3D surface construction algorithms", **Computer graphics**, Vol 21, No. 4, PP 38-44.

Louis, P. and Gokhale, A.M.(1995). "Application of Image Analysis for Characterization of Spatial Arrangement of Features in Microstructures", **Metallurgical and Materials Transactions**, Vol. 26A PP. 1449-1456.

Louis, P. and Gokhale, A.M.(1996). "Computer Simulation of Spatial Arrangement and Connectivity of Particles in Three- Dimensional Microstructure: Application to Model Electrical Conductivity of Polymer Matrix Composite", **Acta Metallurgica et Materiallia**, Vol.44, PP. 1519-1528.

Lubarda, V.A. and Krajcinovic. (1993). Damage Tensors and the Crack Density Distribution. **Int. J. Solids Structures**, Vol. 30, No.20, pp2859-2877.

Malvern, L.E., Jenkins, D.A., Dehoff, R.T. (1992). Rate and Confinement Effects on Cracking and Failure in Uniaxial Compression of Concrete.

Mandelbrot, B.B. and Passoja, D.E. (1984). "Fractal Characteristics of Fracture Surfaces in Metals", **Nature**, Vol.308, PP. 721-722.

Marusin, S.L. (1995). Sample Preparation-the Key to SEM Studies of Failed Concrete. **Cement and Concrete Composites**, Vol.17, pp.311-318.

Nakasa, K. and Nakatsuka, J.I. (1994). Analysis of Crack Branching Morphology in A Disk of Brittle Material Under Axisymmetric Tension by Using Branching Dimension. **Engineering Fracture Mechanics**, Vol. 47, No.3, pp403-415.

Nemati, K.M., Monteiro, J.M. and Scrivener, K.L. (1995). Analysis of Compressive Stress-Induced Cracks in Concrete. **ACI Materials Journal**, Vol. 60, pp.617-630.

Rhines, F.N. and Craig, K.R.(1976). "Measurement of Average Grain Volume and Topological Parameters by Serial Section Analysis", **Metall. Trans.**, Vol. 7A, PP. 1729-1734.

Sabella, P. (1988). "A rendering algorithm for visualizing 3D scalar fields", **Computer Graphics**, Vol 22, No- 4, PP 51-8.

Saltykov, S.A.(1958). Stereometric Metallography, Metallurgizdat, Moscow.

Smith, C.S. and Guttman, L. (1953). **Trans. AIME**, Vol.197, PP.81-86.

Stroven, P. (1976). Application of Various Stereological Methods to the Study of the Grain and the Crack Structure of Concrete. **Journal of Microscopy**, Vol. 107, Part 3, pp313-321.

Taylor, L.M. and Chen, E.P.(1986). Microcrack-Induced Damage Accumulation in Brittle Rock under Dynamic Loading. **Computer Methods in Applied mechanics and Engineering**, Vol. 55, pp.301-320.

Tewari, A., Dighe, M.D. and Gokhale, A. M.(1998) "Estimation of Nearest Neighbor Distance Distribution of Pores in Cast Microstructures", **Materials Characterization**, Vol. 40, PP.119-132.

Tewari, A. (1999). "Effect of Microgravity on Evolution of Microstructure During Liquid Phase Sintering", **Ph.D. dissertation**, Georgia Institute of Technology, Atlanta, GA..

Tewari, A., Gokhale, A.M. and . German, R.M. "Effect of Gravity on Evolution of Three-Dimensional Coordination Number Distribution in Liquid Phase Sintered Microstructures of W-Ni-Fe Alloy", **Acta Materialia**, in press.

Tewari, A. and Gokhale, A.M. "Application Digital Image Processing for Reconstruction of Three Dimensional Microstructure", **Materials Characterization**, in press.

Underwoood, E.E.(1970). Quantitative Stereology, Addison-Wesley, Reading. Mass.

Wang, L.B., Lai, J. S, and Frost, J.D. (1997). *Fourier Morphological Descriptors of Aggregate Profiles.* 2nd international Conference on Image Technology Applications in Civil Engineering, 1997, Sweden.

Wang, L.B., Frost, J.D. and Lai, J. S. (1999). *Non-invasive Strain Measurement of Permanent Deformation Resulted from Rutting*. TRR No.1687, pp85-94.

Yang, S., Tewari, A. and Gokhale, A.M.(1997). "Modeling of Non-Uniform Spatial Arrangement of Fibers in a Ceramic Matrix Composite", **Acta Materiallia**, Vol.45, PP. 3059-69.

Yang, S., Tewari, A. and Gokhale, A.M.(1996). "An Experimental Method for Quantitative Characterization of Spatial Distribution of Fibers in Composites", in **Developments in Materials Characterization Technologies**, eds. G.F. Vander Voort and J.J. Frial, ASM International, Materials Park, Ohio, PP. 33-43.

Zhang, B. (1998). Relationship between Pore Structure and Mechanical Properties of Ordinary Concrete under Bending Fatigue. **Cement and Concrete Research**, Vol. 28, No.5, pp699-711.